Nonlinear integral coupling for synchronization in networks of nonlinear systems

Pavlov, Alexey; Steur, Erik; van de Wouw, Nathan

DOI
10.1016/j.automatica.2022.110202

Publication date
2022

Document Version
Final published version

Published in
Automatica

Automatica 140 (2022) 110202

Contents lists available at ScienceDirect

Automatica

journal homepage: www.elsevier.com/locate/automatica

Nonlinear integral coupling for synchronization in networks of nonlinear systems☆

Alexey Pavlov [a,*], Erik Steur [b,c], Nathan van de Wouw [d,e]

[a] Norwegian University of Science and Technology, Department of Geoscience and Petroleum, NO-7491, Trondheim, Norway
[b] Eindhoven University of Technology, Department of Mechanical Engineering and Institute for Complex Molecular Systems, Eindhoven, The Netherlands
[c] Delft University of Technology, Delft Center for Systems and Control, Delft, The Netherlands
[d] Eindhoven University of Technology, Department of Mechanical Engineering, Eindhoven, The Netherlands
[e] University of Minnesota, Department of Civil, Environmental and Geo-Engineering, Minneapolis, USA

ARTICLE INFO

Article history:
Received 29 April 2019
Received in revised form 11 July 2021
Accepted 4 January 2022
Available online 9 March 2022

Keywords:
Synchronization
Nonlinear systems
Nonlinear couplings
Variable interconnection network
Incremental feedback passivity
Relaxed balanced coloring

ABSTRACT

This paper presents a novel approach to (controlled) synchronization of networked nonlinear systems. For classes of identical single-input–single-output nonlinear systems and networks, including oscillator networks, we propose a systematic design procedure (with generic as well as constructive conditions) for specifying nonlinear coupling functions that guarantee global asymptotic synchronization of the systems' (oscillatory) states. The proposed coupling laws are in the form of a definite integral of a nonlinear "coupling gain" function. It can be fit to the system's nonlinearities and, thus, can avoid cancelling nonlinearities by feedback or high-gain arguments commonly needed for linear (diffusive) coupling laws. As demonstrated by two examples, including a network of FitzHugh–Nagumo oscillators, this design can result in much lower synchronizing coupling gains than for the common case of linear couplings, therewith increasing energy efficiency of the coupling laws and reducing output-noise sensitivity. The resulting coupling structure can be of a varying type, when couplings are activated/deactivated depending on the systems' outputs without undermining overall synchronization. The approach is based on a novel notion of incremental feedback passivity with a nonlinear gain. In addition to the design contribution, these results provide a new insight into potential synchronization mechanisms in natural and artificial nonlinearly coupled systems.

1. Introduction

Synchronization of oscillatory systems and, in particular, of chaotic systems is a phenomenon that received huge attention in scientific literature for the last 20 years (Strogatz, 2003). The co-existence of complex, chaotic or "irregular" dynamics of relatively simple systems on the one hand, and the possibility of some kind of "order" or synchrony in such interconnected systems, on the other hand, forms an intriguing combination for specialists in physics, mathematics, control, neuroscience and biology, thus generating a seemingly endless sequence of various results on this subject. This interest is also explained by a number of applications, already implemented or potential, of synchronization phenomena in various fields of science and technology, see, e.g., Abrams, Pecora, and Motter (2016), Belykh and Porfiri (2016), Caroll and Pecora (1991), Fradkov and Pogromsky (1998), Levine (2004), Nijmeijer and Rodriguez-Angeles (2003), Strogatz (2003) and Oud and Tyukin (2004).

When considering synchronization phenomena in interconnected systems, one can distinguish two directions: synchronization *analysis* of interconnected systems with *given* couplings and interconnection structure, and *design* of interconnection couplings that guarantee systems synchronization (in a certain sense). The last problem, called the *controlled synchronization problem*, is also closely related to several control problems such as observer design and the output regulation problem, see, e.g., Nijmeijer and Mareels (1996) and Pavlov, van de Wouw, and Nijmeijer (2005) for links between these problems.

There is an extensive literature on synchronization and controlled synchronization of *linearly* coupled (nonlinear) systems, where synchronization is to be understood as asymptotic convergence of the states of the interconnected systems to each

☆ This work was partly supported by ITMO University, St. Petersburg, Russia during part-time employment of the first author in 2018-2019. The material in this paper was partially presented at the 5th IFAC Conference on Analysis and Control of Chaotic Systems, October 30 - November 1, 2018, Eindhoven, The Netherlands. This paper was recommended for publication in revised form by Associate Editor Nikhil Chopra under the direction of Editor Daniel Liberzon.

* Corresponding author at: Norwegian University of Science and Technology, Department of Geoscience and Petroleum, NO-7491, Trondheim, Norway.
E-mail addresses: alexey.pavlov@ntnu.no (A. Pavlov), e.steur@tue.nl (E. Steur), n.v.d.wouw@tue.nl (N. van de Wouw).

https://doi.org/10.1016/j.automatica.2022.110202

other, cf. Gambuzza and Frasca (2019), Liu and Chopra (2012), Stan and Sepulchre (2007), Stoorvogel, Saberi, and Zhang (2017), Tuna (2017) and Zhang, Trentelman, and Scherpen (2014). Although for some classes of nonlinear systems, e.g. Euler–Lagrange systems (Nijmeijer & Rodriguez-Angeles, 2003), specific structure of nonlinearities is exploited to design synchronizing linear couplings, for generic nonlinear systems, specific nonlinearities are commonly ignored, as synchronization by linear (diffusive) coupling can often only be guaranteed by suppressing them using high-gain designs (Pogromsky, 1998; Zhang et al., 2014).

Nonlinear couplings provide a greater degree of flexibility. They have been studied, in the scope of synchronization, in He and Yang (2008) and Liu and Chen (2008), in the context of mechanical oscillators (Ramirez, Olvera, Nijmeijer, & Alvarez, 2016), power networks (Dörfler, Chertkov, & Bullo, 2013), neuronal networks (Belykh & Hasler, 2011) and generic phase-oscillators (Dörfler & Bullo, 2014; Strogatz, 2000), with this list being definitely incomplete. See also Fazlyab, Dörfler, and Preciado (2017), Liu and Iwasaki (2017), Nishikawa and Motter (2006) for results on the design (or optimization) of the interaction topology for synchronization of nonlinearly coupled systems. For (first- and second-order) integrator networks, nonlinear couplings have been employed in Andreasson, Dimarogonas, Sandberg, and Johansson (2014) and Saber and Murray (2003) to achieve consensus – a form of synchronization in which all systems converge to the same constant steady state, see also (Yu, Chen, & Cao, 2011; Yu, Chen, Cao, & Kurths, 2010) for the first- and second-order consensus problems for systems with nonlinear dynamics. Greater flexibility of nonlinear couplings makes them particularly interesting for design of couplings to achieve consensus and flocking of multi-robot systems, in particular, for collision avoidance and preserving connectivity, cf. Dimarogonas and Kyriakopoulos (2008), Ji and Egerstedt (2007) and Poonawala and Spong (2017) and the references therein.

Common ways of handling nonlinearities in synchronizing systems include changing/cancelling nonlinearities by feedback to achieve a desired system form or properties (e.g. passivity) (Arcak, 2007; Chopra & Spong, 2008), suppressing nonlinearities by high-gain couplings (Pogromsky, 1998), ensuring synchronization through absolute stability arguments (Proskurnikov, 2013) or achieving synchronization or consensus by various methods, e.g. passivity, with synchronization-error feedback couplings, linear or nonlinear, e.g. Arcak (2007) and Yu et al. (2011, 2010).

Most of the works dealing with synchronization of nonlinear systems focus on *attaining* synchronization (or consensus). The practically important questions of transient and steady-state *performance* of the overall synchronizing interconnected system, energy efficiency of the coupling laws and their sensitivity to noise, remain mostly unaddressed. While for linear systems there is a well-developed machinery to address these questions, see, e.g., Liu, Saberi, Stoorvogel, and Nojavanzadeh (2020) and references therein, for nonlinear systems the problem is much more complex and very few works addressing performance of nonlinear synchronizing systems exist, see, e.g., El-Gohary (2006), Macellari, Karayiannidis, and Dimarogonas (2017) and Modares, Lewis, Kang, and Davoudi (2018). Nonequilibrium steady-state dynamics, as in the problem of synchronization of oscillatory systems, makes the problem even more challenging.

Performance optimization in nonlinear synchronizing systems is directly linked to finding the range of coupling laws that yield synchronization. This range can often be characterized by the lowest and highest (in a certain sense) coupling gains. In synchronization problems it is often only the lower bound that needs to be found, as all gains higher than that bound would yield synchronization. Couplings/controls with gains at this lower bound often lead to lower sensitivity to measurement noise and higher energy efficiency in attaining and maintaining synchronization. On the other hand, finding synchronizing coupling laws with minimal gains can increase our understanding of the system dynamics and reveal novel synchronization mechanisms.

Finding synchronizing coupling laws with minimal gains, as the first step towards performance optimization/analysis of nonlinear synchronizing systems, is the question that motivates our study. For nonlinear systems, minimal synchronizing couplings should generically be nonlinear. Nonlinear coupling laws can be considered as couplings with varying gains. They can fully utilize the intrinsic system dynamics: the gains should generically be low, or even zero, where dynamics is favorable to synchronization, and increase/be nonzero only in those parts of the state space, where system nonlinearities act against synchronization. This observation calls for research in finding minimal couplings, as it excludes most of the coupling laws studied in the literature: linear and nonlinear couplings being functions of the synchronization error e only, cf. Dörfler and Bullo (2014) and Strogatz (2000)—such couplings do not distinguish different parts of the state space, as long as the synchronization error e remains the same.

In the light of the above exposition of the existing literature, the current paper takes on the following combined open challenge: how to design nonlinear coupling laws that (1) achieve synchronization in networks of nonlinear systems (including oscillatory systems), (2) achieve this synchronization through nonlinear couplings that exploit system nonlinearities where they help synchronization and counteract nonlinearities where they act against synchronization, (3) provide performance improvements over conventional, e.g., linear, coupling laws.

1.1. Contributions

We present a systematic approach to the problem of *design* of nonlinear coupling functions to establish synchronization in networks of identical nonlinear single-input–single-output systems. Synchrony is here to be understood as the asymptotic match of the states of the systems, while the nonlinear systems are allowed to exhibit complex *oscillatory (even chaotic)* intrinsic dynamics. The presented approach allows one to find nonlinear couplings with minimal gains (understood in a nonlinear sense to be clarified later) that are tailor-made to system's nonlinearities — both helping and counteracting synchronization depending on the location of the system in its state-space.

The proposed couplings are of the form of a definite integral of some non-negative weight function (or, as we call it, *a nonlinear gain* – the main design parameter) with the limits being the outputs of the systems. This type of coupling has a greater degree of flexibility not only compared to linear (diffusive) couplings, but also compared to arbitrary nonlinear couplings depending only on the synchronization error. It enables variable coupling gains in different parts of the state space — the flexibility essential for finding coupling gains tailor-made to system's nonlinearities.

To formalize in which part of the state space and to what extent system nonlinearities act against synchronization, we introduce the novel notion of *incremental feedback passivity with a nonlinear gain*. The minimal nonlinear integral coupling is then selected to counteract system nonlinearities only in these counter-synchronization parts of the state space, while being zero in the parts where system dynamics render synchronization naturally.

To extend nonlinear integral couplings from 2 to N interconnected systems with a fixed communication graph, we develop new analysis and design tools, as conventional methods based on analysis of the Laplacian matrix do not apply to couplings with gains that can be zero over large parts of the state space. Based on these tools, we present a class of networks – characterized by the

existence of hierarchies of synchronization subspaces, expressed in terms of relaxed balanced coloring and sequential decoloring of the network graph – which support synchronization via nonlinear integral coupling in its full potential.

We demonstrate by two examples that the proposed nonlinear integral couplings can render synchronization by lower input energy (understood in the L_2 sense of the coupling input functions), and with less sensitivity to measurement noise compared to the minimal *linear* coupling laws that guarantee the same rate of convergence. For the example with FitzHugh–Nagumo oscillators, the proposed integral couplings lead to a novel type of synchronization: the couplings are zero most of the time and synchronization is achieved and maintained by spikes in the nonlinear coupling gains. This result can be interesting in neuroscience, where most of the communication happens via spikes.

The developed generic framework is supplied with constructive results leading to verifiable conditions and concrete design procedures for a class of nonlinear systems. This paper extends our initial results reported in Pavlov, Steur, and van de Wouw (2009) and Pavlov, Proskurnikov, Steur, and van de Wouw (2018): the new results are less conservative, exploit the full potential of the nonlinear coupling functions in networks, and are supplied with examples demonstrating novel phenomena.

1.2. Organization

In Section 2, we state the problem of controlled synchronization and introduce nonlinear integral couplings. We also present a simple example that demonstrates the potential of the proposed type of coupling in comparison to the conventional linear coupling functions. In Section 3 we introduce *incremental feedback passivity with a nonlinear gain*—the notion central in the design and analysis of systems interconnected through integral couplings. In that section we also present constructive conditions for verifying this property for a class of nonlinear systems. Section 4 covers synchronization of two systems interacting via nonlinear integral coupling. Extension of these results to synchronization of multiple networked systems is presented in Section 5, where we define the class of networks and the main result on synchronization in such networks with nonlinear integral couplings. Section 6 illustrates the developed theory with an application to synchronization of FitzHugh–Nagumo oscillators, which represent simplified models of neuron dynamics and are a benchmark in the study of synchronization of nonlinear oscillators. Conclusions are drawn in Section 7.

2. Controlled synchronization problem

In this paper we consider N identical nonlinear systems of the form[1]

$$\dot{x}_i = f(x_i, t) + Bu_i,\ \ y_i = Cx_i,\ \ i = 1, \dots, N,\ \ t \geq 0 \tag{1}$$

with $x_i \in \mathbb{R}^n$, $y_i, u_i \in \mathbb{R}$, continuously differentiable in x and piecewise-continuous in t function $f(x, t)$ and vectors $B, C^T \in \mathbb{R}^n$. We assume that $f(x, t)$ satisfies the following technical condition: $\sup_{t\geq 0} |f(0, t)| < +\infty$. The problem of controlled synchronization studied in this paper is to find control laws for each u_i that guarantee

A. boundedness of solutions of the interconnected systems.[2]
B. asymptotic synchronization of the systems' states:

$$|x_i(t) - x_j(t)| \to 0, \quad \text{as} \quad t \to \infty, \quad \forall i, j. \tag{2}$$

For each system i, u_i is allowed to depend on the system's output y_i and on the outputs of neighboring systems that can communicate to system i. In addition, it is required that for identical outputs $y_1 = y_2 = \cdots = y_N$, the controls satisfy $u_1 = u_2 = \cdots = u_N = 0$, such that in exact synchrony the systems exhibit the (oscillatory) dynamics of the unforced systems in (1). The set of systems that can communicate to system i is denoted by $\mathcal{N}_i$. For $i = 1, \dots, N$, these sets define communication graph $\mathcal{G} = (\mathcal{V}, \mathcal{E})$, where $\mathcal{V} = \{1, \dots, N\}$ is the set of nodes, which represent the systems (1), and $\mathcal{E} \subset \mathcal{V} \times \mathcal{V}$ is the set of edges.

2.1. Motivating example

Let us demonstrate the main idea put forward in this paper (namely that of using nonlinear integral couplings) with a simple example of synchronization of two scalar systems given by

$$\dot{y}_1 = y_1 - \frac{1}{3}y_1^3 + G(t) + u_1, \quad \dot{y}_2 = y_2 - \frac{1}{3}y_2^3 + G(t) + u_2,$$

with a bounded piecewise-continuous excitation term $G(t)$. The approach developed in this paper, can be demonstrated by representing the system dynamics in an equivalent form: $\dot{y}_1 = \int_0^{y_1}(1 - s^2)ds + G(t) + u_1$, $\dot{y}_2 = \int_0^{y_2}(1 - s^2)ds + G(t) + u_2$. Then the integral coupling $u_1 = -u_2 = \int_{y_1}^{y_2} \lambda(s)ds$ gives the following error dynamics, with the synchronization error defined as $e := y_1 - y_2$:

$$\dot{e} = \int_{y_2}^{y_1} (\underbrace{1 - s^2 - 2\lambda(s)}_{=:\psi(s)})ds = \psi(\xi)e, \tag{3}$$

where $\xi(y_1, y_2) \in (y_1, y_2)$ results from the mean value theorem. By designing $\lambda(s)$ we can ensure that $\psi(s) \leq -\varepsilon$ for some $\varepsilon > 0$ and all $s \in \mathbb{R}$. Thus, for $V(e) = 1/2e^2$, we have $\dot{V} = 2\psi(\xi)V \leq -2\varepsilon V$, which guarantees exponential synchronization, provided that solutions of the closed-loop system are defined and bounded for all $t \geq 0$. The latter condition needs to be proven separately.

The design of $\lambda(s)$ can be done in different ways:

- $\lambda(s) \equiv K := 1/2 \sup_{s\in\mathbb{R}}(1 - s^2 + \varepsilon) = 1/2(1 + \varepsilon)$ gives linear coupling;
- $\lambda(s) = 1/2(1 - s^2 + \varepsilon)$ cancels the systems dynamics (feedback linearizing coupling) and imposes linear GES error dynamics $\dot{e} = -\varepsilon e$;
- $\lambda(s) \geq 1/2 \max\{1 - s^2 + \varepsilon, 0\}$ cancels the system dynamics only in the area where they act against synchronization and does nothing in the areas where synchronization occurs naturally.

These three choices are illustrated in Fig. 1.[3] The last approach, while providing synchronization with the same guaranteed convergence rate as for the other two approaches, has several favorable properties. Namely, for $\lambda(s) = 1/2 \max\{1 - s^2 + \varepsilon, 0\}$: (1) the coupling law is more energy-efficient since it avoids coupling actions in the areas where synchronization is naturally

[1] General results presented in this paper also hold for systems of the form $\dot{x}_i = f(x_i, u_i, t)$, $y_i = h(x_i)$ under an additional condition that $|\partial h/\partial x(x)| \leq C_h$ for some $C_h > 0$ and all $x \in \mathbb{R}$. For simplicity of presentation we have chosen a less generic form (1).

[2] Boundedness of solutions is a natural and desired property in many applications. Moreover, if overlooked, it may even undermine the validity of proof of asymptotic synchronization, as demonstrated in Proskurnikov and Cao (2017).

[3] As it will be seen from technical results and examples presented further in the paper, the nonlinear integral coupling does not necessarily have to consist of a combination of a feedback-linearizing coupling and a zero coupling, as it is the case for the example presented in Fig. 2.

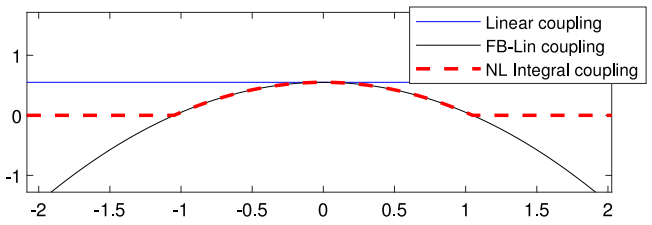

Fig. 1. Gain functions $\lambda(s)$ for linear-, feedback linearization-based and nonlinear integral couplings.

achieved by the system dynamics (in our case, where both y_1 and y_2 lie in the area where $\lambda(s) \equiv 0$: for $y_1, y_2 > \sqrt{1+\varepsilon}$ or $y_1, y_2 < -\sqrt{1+\varepsilon}$). (2) Since $\lambda(s) \in L_1$, then the coupling actions are always bounded by $|u_{1,2}(t)| \leq \int_{-\infty}^{+\infty} \lambda(s)ds$. (3) It has a lower coupling gain (if we define the coupling gain as $g = \int_{y_1}^{y_2} \lambda(s)ds/(y_2 - y_1)$, as in Pavlov et al. (2009)) than for the other two approaches. The lower coupling gain generically gives lower sensitivity to measurement noise on the measured outputs y_1 and y_2. Notice that these favorable properties do not hold for the other two approaches. Moreover, they cannot be achieved by couplings of the form $u = \phi(y_2 - y_1)$ often studied in the literature, cf. Dörfler and Bullo (2014) and Strogatz (2000), as these couplings do not distinguish between different locations of the output variables y_i.

These benefits are illustrated through simulations for $G(t) = 3\sin t$ in Fig. 2, which also includes a comparison to synchronization by the linear coupling with the minimal gain $K = 1/2(1+\varepsilon)$. As can be seen from the figure, nonlinear integral coupling yields synchronization by lower coupling values, with lower sensitivity to measurement noise (both in controls and steady-state synchronization error), and with higher energy efficiency. Over the simulated period, the L_2 norms of input signals for the linear and nonlinear integral couplings are equal to $\|u_i^{Lin}\|_{L_2} = 1.12$, $\|u_i^{NLin}\|_{L_2} = 0.35$.

Note that although the nonlinear integral coupling yields the same guaranteed synchronization rate characterized by ε, its actual convergence rate for the given initial conditions can be lower than for the case of linear coupling. By designing a larger gain function $\lambda(s) \geq 1/2\max\{1 - s^2 + \varepsilon, 0\}$, which is the intrinsic property of the method, one can improve the transient convergence rate, yet at the expense of increased sensitivity to the measurement noise and decreased energy efficiency. The possibility of such a trade-off between convergence rate and noise sensitivity/ energy efficiency (at lower coupling gains) is the flexibility not present in the case of linear couplings: the constant coupling gains needed for the guaranteed convergence rate ε are lower bounded by $K = 1/2(1+\varepsilon)$.

In the remainder of the paper we investigate the application of nonlinear integral coupling of the form $u = \int_{y_i}^{y_j} \lambda(s)ds$ to ensure synchronization of N n-dimensional nonlinear systems coupled through a communication network with a fixed topology. Our motivation is to design synchronizing couplings with lower gains and better performance properties compared to the standard methods of linear and nonlinear couplings based on error feedback only, and nonlinear couplings based on feedback linearization. We are interested both in generic conditions under which one can find such integral nonlinear couplings (both on the level of the system dynamics, as well as on the level of communication network topology) and in constructive conditions for specific classes of nonlinear systems.

2.2. Nonlinear integral coupling

Below, we give a formal definition of nonlinear integral coupling between dynamical systems.

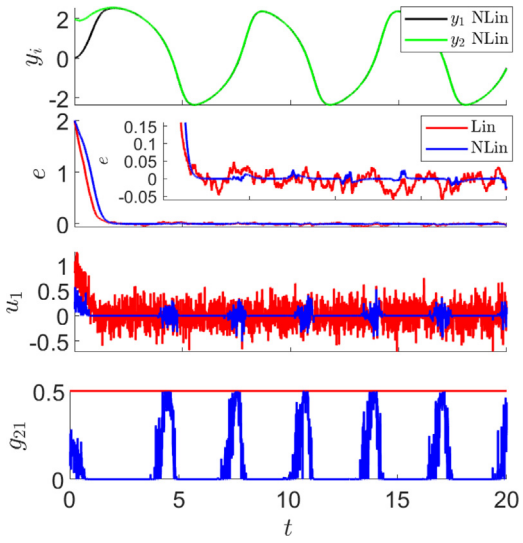

Fig. 2. Simulation results for synchronization with measurement noise for nonlinear integral coupling, $\varepsilon = 0.001$, $y_1(0) = 2, y_2(0) = 0$ – plot 1. Comparison with synchronization by linear coupling with the gain $K = 1/2(1+\varepsilon)$ – plots 2–4 for synchronization error e, coupling value u_1 and coupling gain g.

Definition 1. Given N systems with a communication topology specified by the graph $\mathcal{G}$ with the corresponding sets of neighboring nodes $\mathcal{N}_i$, $i = 1, \ldots, N$, we say that systems are interconnected through integral coupling with a nonlinear coupling gain $\lambda(s) \geq 0$, $\forall s$, if

$$u_i = \sum_{j \in \mathcal{N}_i} \int_{y_i}^{y_j} \lambda(s)ds, \quad i \in \mathcal{V}. \tag{4}$$

This kind of coupling satisfies the requirement that for identical outputs the coupling must be zero, since for $y_i = y_j$ $\forall i, j \in \mathcal{V}$, we have $u_i = 0$. Notice that for $\lambda(s) \equiv K = Const > 0$, the nonlinear integral coupling (4) represents linear diffusive coupling $u_i = K\sum_{j \in \mathcal{N}_i}(y_j - y_i)$, $i \in \mathcal{V}$ as a special case, which is well studied in literature, see, e.g. Fradkov and Pogromsky (1998), Gambuzza and Frasca (2019), Liu and Chopra (2012), Pogromsky (1998), Stan and Sepulchre (2007), Stoorvogel et al. (2017) and Zhang et al. (2014).

3. Incremental feedback passivity

In this section, we present the definition, some properties and constructive conditions for incremental feedback passivity (iFP) with a nonlinear gain, which is the key property for synchronization analysis in this paper. It is an extension of the incremental passivity property employed in various works within nonlinear systems and control, see, e.g. Pavlov and Marconi (2008) and Stan and Sepulchre (2007).

3.1. Incremental feedback passivity with nonlinear gain

Definition 2. System (1), for $N = 1$, is called incrementally feedback passive with nonlinear gain $\gamma(s) \geq 0$ – denoted as *iFP*$(-\gamma(s))$ – if there exists a C^1 function $S(x) : \mathbb{R}^n \to \mathbb{R}_+$ and a function $\rho(x) : \mathbb{R}^n \to \mathbb{R}_+$ such that for any two inputs $u_a(t)$ and $u_b(t)$ any two solutions $x_a(t)$, $x_b(t)$ of system (1), for $N = 1$, corresponding to these inputs, with outputs y_a and y_b, satisfy the inequality

$$\frac{d}{dt}S(x_a(t) - x_b(t)) \leq -\rho(x_a - x_b) + (y_a - y_b)\left(\int_{y_b}^{y_a} \gamma(s)ds + u_a - u_b\right). \tag{5}$$

If $\rho(x)$ is positive definite, we call system (1), for $N = 1$, incrementally strictly feedback passive with nonlinear gain $\gamma(s)$. It is denoted by the acronym *iSFP*$(-\gamma(s))$.

For $\gamma(s) \equiv 0$ we obtain the standard definition of incremental passivity. For $\gamma(s) \geq 0$, system (1) can be made incrementally passive by feedback transformation $u = \int_y^{p(t)} \lambda(s)ds + v$, for some integrable function $\lambda(s) \geq \gamma(s)$, $\forall s \in \mathbb{R}$, arbitrary continuous function $p(\cdot)$ and v, which is a new input after the transformation. In this case, for two outputs y_a and y_b, the corresponding u_a and u_b will satisfy $u_a - u_b = \int_{y_a}^{y_b} \lambda(s)ds + v_a - v_b$. This difference multiplied by $(y_a - y_b)$ dominates the positive term $(y_a - y_b)\int_{y_b}^{y_a} \gamma(s)ds$ in (5). Thus, for the two solutions $x_a(t)$, $x_b(t)$ corresponding to these u_a and u_b, we have

$$\frac{d}{dt}S(x_a(t) - x_b(t)) \leq -\rho(x_a - x_b) + (y_a - y_b)(v_a - v_b),$$

i.e., the system is incrementally passive with respect to the new input v.[4] For the synchronization analysis in this paper, we require an additional assumption on $S(x)$ and $\rho(x)$.

Assumption 1. System (1), for $N = 1$, has the *iSFP*$(-\gamma(s))$ property with the functions $S(x)$ and $\rho(x)$ from (5) satisfying

$$\alpha_1(|x|) \leq S(x) \leq \alpha_2(|x|), \tag{6}$$

$$\left|\frac{\partial S}{\partial x}(x)\right| \leq C_S|x|, \tag{7}$$

$$\rho(x) \geq |x|\kappa(|x|), \tag{8}$$

for some $C_S > 0$ and class-$\mathcal{K}_\infty$ functions[5] $\alpha_1(\cdot)$, $\alpha_2(\cdot)$, and $\kappa(\cdot)$.

This assumption holds, for example, for quadratic positive definite $S(x) = x^TPx$ and $\rho(x) = x^TRx$. An important secondary property of *iSFP*$(-\gamma(s))$ systems (1) is given in the following lemma (see the proof in the Appendix). For notational convenience, in this lemma we omit the subscript i from the state x and control u.

Lemma 1. *Suppose system (1) has iSFP*$(-\gamma(s))$ *property with $S(x)$ and $\rho(x)$ satisfying Assumption 1 and $\gamma(s) \geq 0$ satisfying $\int_{-\infty}^{+\infty} \gamma(s)ds =: C_\gamma < +\infty$. Let the control $u = u(x, t)$ satisfy $|u(x, t)| \leq C_u$, $\forall x, t$ and some $C_u > 0$. Then, any solution of the closed-loop system lies in a compact positively invariant set for all $t \geq 0$.*

3.2. Constructive conditions

All subsequent results on synchronization are formulated in terms of the *iSFP*$(-\gamma(s))$ property. In this section, we provide constructive results on how to verify this property and to find $\gamma(s)$ in (5) for systems of the form (1). All the proofs can be found in the Appendix.

Theorem 1. *Suppose there exist $P = P^T > 0$, $R = R^T \geq 0$ and a scalar continuous function $\tilde{\gamma}(s)$ such that*

$$P\frac{\partial f}{\partial x}(x, t) + \frac{\partial f^T}{\partial x}(x, t)P - 2C^TC\tilde{\gamma}(Cx) \leq -R \ \forall x \in \mathbb{R}^n,$$
$$PB = C^T, t \geq 0 \tag{9}$$

Then system (1) is iFP$(-\gamma(s))$ *with $\gamma(s) = \max\{0, \tilde{\gamma}(s)\}$, $S(x) = 1/2x^TPx$ and $\rho(x) = 1/2x^TRx$ (see (5)). If $R > 0$, then system (1) is iSFP*$(-\gamma(s))$ *with functions $S(x)$ and $\rho(x)$ satisfying Assumption 1.*

This result can be made more constructive (see Theorem 2 below) for the following class of systems:

$$\dot{z} = q(z, y, t), \dot{y} = p(z, y, t) + u, \ z \in \mathbb{R}^{n-1}, y, u \in \mathbb{R}, t \geq 0 \tag{10}$$

where $q(z, y, t)$ and $p(z, y, t)$ are continuously differentiable in (z, y) and piecewise continuous in t. Notice that this system is of the form (1) with $x = [z^T, y]^T$, $f(x, t) = [q^T, p]^T$, $B = [\mathbf{0}^T, 1]^T$ and $C = [\mathbf{0}^T, 1]$.

Theorem 2. *Consider system (10). Suppose there exist $(n-1) \times (n-1)$ matrices $Q = Q^T > 0$ and $M = M^T > 0$ such that inequality*

$$Q\frac{\partial q}{\partial z}(z, y, t) + \frac{\partial q^T}{\partial z}(z, y, t)Q \leq -M \tag{11}$$

holds for all (z, y) and $t \geq 0$. Let $\tilde{\gamma}(y)$ satisfy

$$\tilde{\gamma}(y) \geq \epsilon + \frac{\partial p}{\partial y} + \frac{1}{2}\left(Q\frac{\partial q}{\partial y} + \frac{\partial p^T}{\partial z}\right)^T (M - \epsilon I_{n-1})^{-1}\left(Q\frac{\partial q}{\partial y} + \frac{\partial p^T}{\partial z}\right) \tag{12}$$

for all (z, y) and some $\epsilon > 0$ satisfying

$$M - \epsilon I_{n-1} > 0, \tag{13}$$

where I_{n-1} is the $(n-1) \times (n-1)$ identity matrix. Then system (10) is iSFP$(-\gamma(s))$ *with $\gamma(s) = \max\{0, \tilde{\gamma}(s)\}$ and quadratic positive definite $S(x)$ and $\rho(x)$ satisfying Assumption 1.*

A function $\tilde{\gamma}(y)$ satisfying (12) can be found if the right-hand side of (12) is independent of z and t or can be bounded from above by a y-dependent function.

Condition (11) guarantees that the zero dynamics of system (10) (i.e., the z-dynamics) are convergent (Pavlov, Pogromsky, van de Wouw, & Nijmeijer, 2004), which implies that for a given function $y(t)$ all solutions of the system $\dot{z} = q(z, y, t)$ converge to a unique bounded globally asymptotically stable steady-state solution determined only by $y(t)$. This property of the zero dynamics can be considered as a specific minimum phase property of the overall system (10).

4. Synchronization of two systems

Below we apply the *iSFP*$(-\gamma(s))$ property to the controlled synchronization problem for two systems.

Theorem 3. *Consider two systems a and b of the form (1) interconnected through the integral coupling:*

$$u_a = \int_{y_a}^{y_b} \lambda(s)ds, \qquad u_b = \int_{y_b}^{y_a} \lambda(s)ds. \tag{14}$$

Suppose (1) is iSFP$(-\gamma(s))$ *with $S(x)$ and $\rho(x)$ satisfying Assumption 1. If $\lambda(\cdot) \in L_1$ and*

$$2\lambda(s) \geq \gamma(s) \tag{15}$$

then all solutions of the closed-loop system (1), (14) are bounded for all $t \geq 0$ and satisfy (2) for $i = a, j = b$.

Proof. Boundedness: The L_1 condition on $\lambda(\cdot)$ and (14) imply that both u_a and u_b satisfy $|u_{a,b}| \leq \|\lambda(\cdot)\|_{L_1}$. The L_1 condition on $\lambda(\cdot)$ together with conditions (15) and $\gamma(s) \geq 0$ (see Definition 2) also imply that $\gamma(\cdot) \in L_1$. Thus, by Lemma 1, both $x_a(t)$ and $x_b(t)$ lie in a compact positive invariant set for all $t \geq 0$.

Synchronization: From (14) we obtain $u_a - u_b = \int_{y_a}^{y_b} 2\lambda(s)ds$. Substituting this expression into (5) and utilizing inequality (15),

[4] Notice that for $\gamma(s) \equiv K$, with K constant, Definition 2 turns into the already known definition of incremental feedback passivity (Hamadeh, Stan, Sepulchre, & Goncalves, 2012), with the linear passifying transformation $u = -Ky + v$.

[5] A function $\alpha : \mathbb{R}_+ \to \mathbb{R}_+$ is a class-$\mathcal{K}_\infty$ function if it is continuous, strictly increasing, $\alpha(0) = 0$ and $\alpha(r) \to \infty$ as $r \to \infty$, cf. Khalil (1996).

we obtain

$$\frac{d}{dt}S(x_a(t)-x_b(t)) \le -\rho(x_a-x_b) \qquad (16)$$
$$+(y_a-y_b)\left(\int_{y_b}^{y_a}\gamma(s)-2\lambda(s)ds\right) \le -\rho(x_a-x_b).$$

Since $x_a(t)$ and $x_b(t)$ belong to a compact set for all $t \ge 0$, by Barbalat's lemma (Khalil, 1996, Section 8.3) we obtain $\rho(x_a(t)-x_b(t)) \to 0$ as $t \to +\infty$. Due to positive definiteness of $\rho(x)$, this implies (2). □

Remark 1. The case of master–slave synchronization, when one of the control inputs in (14) equals zero (e.g., $u_a = \int_{y_a}^{y_b}\lambda(s)ds$, $u_b = 0$) is proven in the same way. In this case, condition (15) is replaced by the condition $\lambda(s) \ge \gamma(s)$, $\forall s \in \mathbb{R}$.

Remark 2. In case if $S(x) = x^TPx$ and $\rho(x) = x^TRx$ for some $P = P^T > 0$ and $R = R^T > 0$, one can easily see that (16) implies exponential synchronization, i.e.:

$$|x_a(t)-x_b(t)| \le \alpha e^{-\beta t}|x_a(0)-x_b(0)|, \quad \forall t \ge 0, \qquad (17)$$

for some $\alpha > 0, \beta > 0$. In this case, one can expect a certain degree of robustness of synchronization against variations in the right-hand sides of individual systems (1) and communication effects such as sampling and time-delays. Depending on how these variations appear in the systems' dynamics, synchronization is achieved either exactly (i.e. the asymptotic match of the systems' states) or *practically* (i.e. the differences in all state-trajectories evolve to a small neighborhood of zero), cf. Panteley and Loría (2017) and Steur and Nijmeijer (2011).

Remark 3. The condition that $\rho(x)$ is positive definite in (5) can be relaxed; In particular, $\rho(x_a-x_b)$ can be substituted by $\rho(y_a-y_b)$, where $\rho(y)$ is a positive definite function. In this case, the conditions in Theorem 3 will guarantee output synchronization: $y_a(t)-y_b(t) \to 0$, as $t \to +\infty$. Full state synchronization can be achieved by the observability condition that $y_a(t)-y_b(t) \to 0$ and $u_a(t)-u_b(t) \to 0$ imply $x_a(t)-x_b(t) \to 0$, as $t \to +\infty$.

5. Synchronization of multiple systems

In this section, we extend the results from the previous section to the case of N systems (1) interconnected through integral coupling (4) with a communication network given by graph $\mathcal{G}$. This task appears to be challenging because of the nonlinear nature of the coupling (4), which prevents the use of standard techniques for synchronization analysis based on analysis of the Laplacian of the network graph. The main difficulty is related to the fact that $\lambda(s)$ is allowed to be zero, thereby leading to regions of output values where nodes lose connectivity. In these regions, it is not the coupling, but the original system dynamics that takes care of synchronization. Synchronization results stemming from absolute stability methods, see, e.g., Proskurnikov (2013, 2014), cannot be applied here given the generic nonlinear nature of both the integral couplings and the system dynamics. The only applicable result in this direction was reported in Pavlov et al. (2018), stating that, for a given $\lambda(s)$ and given network topology with a connected bidirectional communication graph, there exists $k_* > 0$ such that synchronization is achieved through coupling

$$u_i = k\sum_{j\in\mathcal{N}_i}\int_{y_i}^{y_j}\lambda(s)ds, \quad i \in \mathcal{V}, \quad \forall\, k \ge k_*. \qquad (18)$$

That result is more of a qualitative nature, since there are no constructive methods for finding k_*.

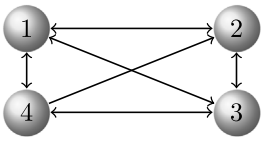

Fig. 3. Example of 4 interconnected systems.

In this section, we provide a method for analyzing synchronization of N systems interconnected through nonlinear integral couplings over directed communication graphs. We firstly explain the idea behind the method with an illustrative example, then we provide the formal method for synchronization analysis of multiple systems interconnected over a given communication graph.

5.1. Illustrative example

Consider a network of 4 systems with *iSFP*($-\gamma(s)$) property satisfying Assumption 1 interconnected through nonlinear integral couplings (4) with the communication graph as in Fig. 3. To demonstrate synchronization of all nodes, let us first consider nodes 1 and 3. The nonlinear integral couplings u_1 and u_3 are given by

$$u_1 = \int_{y_1}^{y_2}\lambda(s)ds + \int_{y_1}^{y_4}\lambda(s)ds + \int_{y_1}^{y_3}\lambda(s)ds \qquad (19)$$
$$u_3 = \int_{y_3}^{y_2}\lambda(s)ds + \int_{y_3}^{y_4}\lambda(s)ds + \int_{y_3}^{y_1}\lambda(s)ds. \qquad (20)$$

Taking into account the fact that $\int_{y_1}^{y_*}\lambda(s) - \int_{y_3}^{y_*}\lambda(s) = \int_{y_1}^{y_3}\lambda(s)ds$, we obtain $u_1-u_3 = \int_{y_1}^{y_3}4\lambda(s)ds$. Substituting this equality in (5), gives

$$\frac{d}{dt}S(x_1(t)-x_3(t)) \le -\rho(x_1-x_3) + (y_1-y_3)\left(\int_{y_3}^{y_1}\gamma(s)-4\lambda(s)ds\right).$$

Therefore, if

$$\Gamma\lambda(s) \ge \gamma(s), \quad \forall s \in \mathbb{R}, \qquad (21)$$

for $\Gamma = 4$, then $\frac{d}{dt}S(x_1(t)-x_3(t)) \le -\rho(x_1-x_3)$, which, by boundedness of solutions and Barbalat's lemma (Khalil, 1996, Section 8.3), implies that $x_1(t)$ and $x_3(t)$ asymptotically synchronize. Applying the same reasoning for nodes 2 and 4, we obtain that these nodes synchronize if (21) holds for $\Gamma = 3$. The difference in Γ from the case of nodes 1, 3 is due to the fact that there is only one link between nodes 2 and 4 compared to two links between 1 and 3. Thus, under condition (21) for $\Gamma = 3$, nodes 1, 3 and 2, 4 form two clusters with synchronizing elements.

Two clusters with synchronizing elements can be merged into a larger synchronizing cluster as can be seen below with clusters $\{1, 3\}$ and $\{2, 4\}$. Consider two nodes from these clusters: 1 and 2. For them, we have

$$u_1 = \int_{y_1}^{y_2}\lambda(s)ds + \int_{y_1}^{y_4}\lambda(s)ds + \int_{y_1}^{y_3}\lambda(s)ds,$$
$$= 2\int_{y_1}^{y_2}\lambda(s)ds + \underbrace{\int_{y_2}^{y_4}\lambda(s)ds + \int_{y_1}^{y_3}\lambda(s)ds}_{=:\epsilon_1(t)\to 0,\ \text{as}\ t\to+\infty} \qquad (22)$$

$$u_2 = \int_{y_2}^{y_1}\lambda(s)ds + \int_{y_2}^{y_3}\lambda(s)ds + \int_{y_2}^{y_4}\lambda(s)ds$$
$$= 2\int_{y_2}^{y_1}\lambda(s)ds + \underbrace{\int_{y_1}^{y_3}\lambda(s)ds + \int_{y_2}^{y_4}\lambda(s)ds}_{=:\epsilon_2(t)\to 0,\ \text{as}\ t\to+\infty} \qquad (23)$$

where the vanishing terms correspond to synchronizing nodes within the two clusters (provided that $\lambda(s)$ is bounded on $\mathbb{R}$). Applying inequality (5) to nodes 1 and 2, together with expressions (22), (23), we obtain

$$\frac{d}{dt}S(x_1(t)-x_2(t)) \leq -\rho(x_1-x_2) + (y_1-y_2)\left(\int_{y_2}^{y_1}\gamma(s)-4\lambda(s)ds\right) + (y_1-y_2)(\epsilon_1(t)-\epsilon_2(t)).$$

For $\lambda(s)$ satisfying (21) with $\Gamma = 4$, this implies

$$\frac{d}{dt}S(x_1(t)-x_2(t)) \leq -\rho(x_1-x_2)+(y_1-y_2)(\epsilon_1(t)-\epsilon_2(t)).$$

It can be demonstrated that since $\epsilon_1(t), \epsilon_2(t) \to 0$, as $t \to +\infty$, under Assumption 1 the last inequality implies that $x_1(t)$ and $x_2(t)$ asymptotically synchronize (for rigorous proofs see subsequent technical results). This leads to synchronization of two clusters $\{1, 3\}$ and $\{2, 4\}$, i.e., synchronization of the overall network.

In our example we sequentially merged nodes and clusters into larger clusters of synchronizing nodes until all nodes in the network are merged in one synchronizing cluster. This process, together with the corresponding values of Γ that guarantee that after each merger, the new cluster will still consist of synchronizing nodes, is described below

$$\begin{aligned}\mathcal{P}_0 &:= \{\{1\},\{2\},\{3\},\{4\}\},\ \Gamma_1 = 4\\ \mathcal{P}_1 &:= \{\{1,3\},\{2\},\{4\}\},\ \Gamma_2 = 3\\ \mathcal{P}_2 &:= \{\{1,3\},\{2,4\}\},\ \Gamma_3 = 4\\ \mathcal{P}_3 &:= \{\{1,2,3,4\}\},\end{aligned}$$

where each partition $\mathcal{P}_i$, $i = 0, \ldots, 3$ consists of either individual nodes or clusters of synchronizing nodes. Note that for $\Gamma = \min_{k=1,2,3}\Gamma_k$, condition (21) will be satisfied also for all Γ_k. Condition (21) with this Γ is our final condition on the nonlinear gain $\lambda(s)$.

For general graphs, this method is applicable under certain conditions on the graph. The idea behind these conditions can be understood from the example above . The key property to ensure merging of two individual nodes a, b ($a, b = 1, 3$ or $a, b = 2, 4$ in our example) into a larger synchronizing cluster is that they have the same external neighbors, i.e. $\mathcal{N}_a\backslash\{a,b\} = \mathcal{N}_b\backslash\{a,b\}$. Furthermore, external neighbors from the same synchronizing cluster (i.e., these have the same asymptotic behavior) can be treated as the same neighboring node (for details, see exact proofs of further technical results in this section). Each merger operation is thus performed on two nodes/clusters that have (asymptotically) the same external neighbors. Graphically, the easiest way to represent this sequential operation is by coloring the nodes and clusters, such that nodes in merged clusters get the same color. This approach is formalized in the next subsection.

5.2. Synchronization analysis by relaxed balanced coloring

Relaxed balanced coloring and related notions presented below provide both a formal framework as well as an algorithmic support for the method demonstrated in the previous subsection. The main result presented in this section provides synchronization conditions for a class of networks – so-called *sequentially decolorable networks* – defined below. We will arrive at this result in three steps: (1) definition of relaxed balanced coloring (it conveniently captures the necessary network partitions into nodes with the (asymptotically) the same neighboring nodes), (2) definitions of color reduction and sequentially reducible networks — the class of networks that allows for sequential merger of synchronizing clusters leading to synchronization of the whole network and (3) the main synchronization result that links nonlinear integral coupling and sequentially decolorable networks.

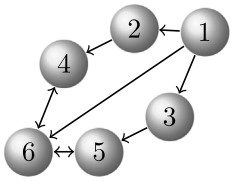

Fig. 4. A communication network graph.

5.2.1. Relaxed balanced coloring

Definition 3. A coloring of the nodes with $k \in \{1, \ldots, N\}$ colors c_1,..., c_k is called a *relaxed balanced coloring* if

- each node is assigned a color, and
- every c_i-colored node receives an equal number of edges from c_j-colored nodes for all $j \in \{1, 2 \ldots, k\}\backslash\{i\}$.

This notion is a relaxation of *balanced coloring*, where each c_i-colored node receives an equal number of edges from c_j-colored nodes for all $j \in \{1, 2 \ldots, k\}$, *and* from the nodes with its own color c_i.[6] It will be shown below that this relaxation is enough for our purposes and that it covers cases not covered by the (non-relaxed) balanced coloring.

A graph can be colored according to relaxed balanced coloring in multiple ways. Each coloring defines the corresponding partitioning of the nodes denoted by $\mathcal{P}_i$. The two trivial colorings are given by (a) assigning each node an individual color and (b) by assigning all nodes the same color. An example of a graph and the corresponding relaxed balanced colorings are presented below.

Example 1. Consider the graph $\mathcal{G}$ shown in Fig. 4. All its relaxed balanced colorings are presented in Fig. 5. The corresponding partitions defined by the colors are:

$$\begin{aligned}\mathcal{P}_0 &:= \{\{1\},\{2\},\{3\},\{4\},\{5\},\{6\}\},\\ \mathcal{P}_1 &:= \{\{1\},\{2,3\},\{4\},\{5\},\{6\}\},\\ \mathcal{P}_2 &:= \{\{1\},\{2,3\},\{4,5\},\{6\}\},\\ \mathcal{P}_3 &:= \{\{1,3\},\{3\},\{4\},\{5\},\{6\}\},\\ \mathcal{P}_4 &:= \{\{1,2\},\{3\},\{4\},\{5\},\{6\}\},\\ \mathcal{P}_5 &:= \{\{1,2,3\},\{4\},\{5\},\{6\}\},\\ \mathcal{P}_6 &:= \{\{1,2,3\},\{4,5\},\{6\}\},\\ \mathcal{P}_7 &:= \{\{1,2,3\},\{4,5,6\}\},\\ \mathcal{P}_8 &:= \{\{1,2,3,4,5,6\}\}.\end{aligned}$$

Suppose that a given graph $\mathcal{G}$ admits K additional relaxed balanced colorings besides the above two trivial ones. Of course, we require these K other relaxed balanced colorings to be distinct in the sense that the partitions corresponding to the relaxed balanced coloring are all different. We then denote the relaxed balanced coloring with N-colors by partitioning $\mathcal{P}_0 = \{\{1\},\{2\},\ldots,\{N\}\}$, the coloring with one color by partitioning $\mathcal{P}_{K+1} = \{\{1,2,\ldots,N\}\}$, and the other relaxed balanced colorings by partitionings $\mathcal{P}_j$, $j = 1, \ldots, K$.

[6] *(Relaxed) balanced coloring* is a common terminology in the analysis of synchronization (in particular, cluster synchronization) (Belykh & Hasler, 2011; Golubitsky, Stewart, & Török, 2005; Steur, Ünal, van Leeuwen, & Michiels, 2016). For the problem considered in this paper, a *relaxed balanced coloring* is equivalent to an *almost equitable partition* (Cardoso, Delorme, & Rama, 2007), which is frequently used in the framework of consensus theory and the analysis of network controllability (Gambuzza & Frasca, 2019; Notarstefano & Parlangeli, 2013).

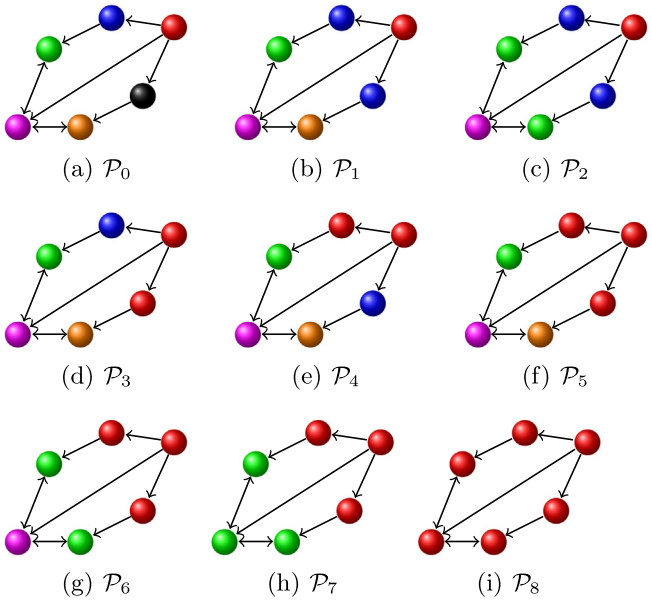

Fig. 5. All balanced colorings of the graph from Fig. 4.

5.2.2. Color reduction

Relaxed balanced colorings can be ordered in a hierarchy by means of *refinement*. Here a partition $\mathcal{P}_i$ of the set $\mathcal{V}$ is a *refinement* of a partition $\mathcal{P}_j$ of $\mathcal{V}$, denoted by $\mathcal{P}_i \subset \mathcal{P}_j$, if every element of $\mathcal{P}_i$ is a subset of some element of $\mathcal{P}_j$. We say that $\mathcal{P}_i$ is *finer* than $\mathcal{P}_j$, and $\mathcal{P}_j$ is *coarser* than $\mathcal{P}_i$. For example, $\mathcal{P}_0$ is finer than $\mathcal{P}_{K+1}$, or, equivalently, $\mathcal{P}_{K+1}$ is coarser than $\mathcal{P}_0$. Clearly, if $\mathcal{P}_i$ is finer (resp. coarser) than $\mathcal{P}_j$, then the relaxed balanced coloring associated to $\mathcal{P}_i$ has more (resp. less) colors than the one associated to $\mathcal{P}_j$. Similar hierarchies have been utilized for analysis of synchrony subspaces (Aguiar & Dias, 2014).

This hierarchy defines multiple "chains" of refinement. For example, the network graph shown in Fig. 4 has multiple chains of refinement, e.g.

$$\mathcal{P}_0 \subset \mathcal{P}_1 \subset \mathcal{P}_2 \subset \mathcal{P}_6 \subset \mathcal{P}_7 \subset \mathcal{P}_8. \tag{24}$$

These chains of refinement can be represented in a diagram called a *Hasse diagram* (Birkhoff, 1948). In this diagram, there is an arrow from $\mathcal{P}_i$ to $\mathcal{P}_j$ (i.e. $\mathcal{P}_i \to \mathcal{P}_j$) if and only if $\mathcal{P}_j \subset \mathcal{P}_i$ and there is no other partition $\mathcal{P}_\ell$ such that $\mathcal{P}_j \subset \mathcal{P}_\ell \subset \mathcal{P}_i$. (The edges in a Hasse diagram are sometimes undirected. We prefer the use of directed edges.) Furthermore, if $\mathcal{P}_i \subset \mathcal{P}_j$, then $\mathcal{P}_j$ appears lower in the diagram than $\mathcal{P}_i$. Consequently, $\mathcal{P}_0$ is at the top of the diagram and $\mathcal{P}_{K+1}$ is at the bottom. For the network graph considered in Example 1 (Fig. 4), the corresponding Hasse diagram is presented in Fig. 6.

Definition 4. A network $\mathcal{G}$ that admits a relaxed balanced coloring $\mathcal{P}_i$ with k_i colors from the set $\mathbf{C}_i = \{c_1, \ldots, c_{k_i}\}$ is *color-reducible* if there exists another relaxed balanced coloring $\mathcal{P}_j$ with $k_j < k_i$ colors from the set $\mathbf{C}_j$ such that

- $\mathbf{C}_j \subset \mathbf{C}_i$;
- for all $\ell = 1, \ldots, k_j$, every c_ℓ-colored node in $\mathcal{P}_i$ has (or can be assigned) the same color in $\mathcal{P}_j$.

Clearly, all possible color reductions starting from a relaxed balanced coloring $\mathcal{P}_i$ are specified by the directed paths in the Hasse diagram with $\mathcal{P}_i$ as the root node. The following result is immediate.

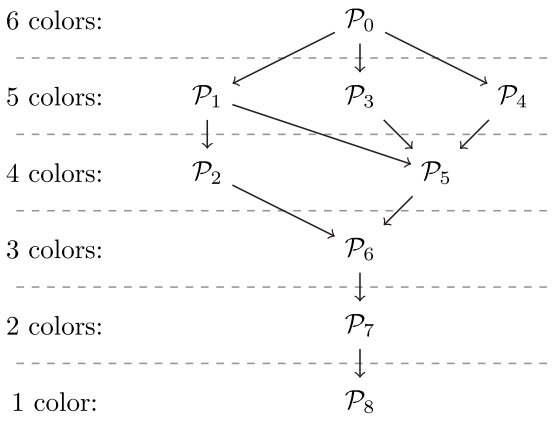

Fig. 6. Hasse diagram for the network graph from Example 1 (Fig. 4) and the corresponding chains of refinement.

Lemma 2. *If the Hasse diagram of relaxed balanced colorings of a graph $\mathcal{G}$ with the operation of refinement contains a directed path of length $N-1$, then there exists a sequence of color reductions from $\mathcal{P}_0$ to $\mathcal{P}_{K+1}$, where in each reduction step exactly one color is removed.*

Definition 5. A network that satisfies the condition of Lemma 2 is called *sequentially decolorable*.

The property that the graph $\mathcal{G}$ is sequentially decolorable is the main condition for synchronization analysis presented further. It can be verified algorithmically. The corresponding MATLAB code is available at Steur (2019).

Note that the existence of a path of length $N-1$ in the Hasse diagram is equivalent to the existence of a chain of refinements

$$\mathcal{P}_0 = \mathcal{P}_{i_1} \subset \mathcal{P}_{i_2} \subset \ldots \subset \mathcal{P}_{i_N} = \mathcal{P}_{K+1} \tag{25}$$

of length $N-1$, with $i_1, i_2, \ldots, i_N \in \{0, 1, 2, \ldots, K+1\}$ (here the length of the chain is understood as the number of symbols $\subset$ in the chain). As can be seen from the Hasse diagram presented in Fig. 6, the network graph from Example 1 (Fig. 4) is sequentially decolorable, with the corresponding chain of refinements given by (24).

The following lemma details the structure of the chain of refinements of length $N-1$ of a sequentially decolorable network (see the Appendix for the proof).

Lemma 3. *Consider a sequentially decolorable network $\mathcal{G}$ with the corresponding chain of refinements (25). In each step from i_k to i_{k+1} in the chain of refinements (25), $\mathcal{P}_{i_{k+1}}$ is obtained from $\mathcal{P}_{i_k}$ by merging two elements:*

$$\begin{aligned} \mathcal{P}_{i_k} &= \mathcal{A}, \mathcal{B}, \mathcal{C}_1, \ldots, \mathcal{C}_l, \\ \mathcal{P}_{i_{k+1}} &= \mathcal{A} \cup \mathcal{B}, \mathcal{C}_1, \ldots, \mathcal{C}_l, \end{aligned} \tag{26}$$

for some $\mathcal{A}, \mathcal{B}, \mathcal{C}_1, \ldots, \mathcal{C}_l$. Moreover, for all $a \in \mathcal{A}$ and $b \in \mathcal{B}$ it holds that

$$|\mathcal{N}_a \cap \mathcal{C}_j| = |\mathcal{N}_b \cap \mathcal{C}_j| \quad \forall j = 1, \ldots, l. \tag{27}$$

Moreover, $|\mathcal{N}_a \cap \mathcal{B}|$, $|\mathcal{N}_b \cap \mathcal{A}|$, $|\mathcal{N}_a \cap \mathcal{C}_j|$ and $|\mathcal{N}_b \cap \mathcal{C}_j|$, $\forall j = 1, \ldots, l$, are independent of the particular choice of $a \in \mathcal{A}$ and $b \in \mathcal{B}$.

Before formulating the main result of this section, let us give the following definition.

Definition 6. Consider a sequentially decolorable network graph $\mathcal{G}$ with the corresponding chain of refinement (25). For each

transition $\mathcal{P}_{i_k} \to \mathcal{P}_{i_{k+1}}$ given in (26), $k = 1, \ldots, N-1$, define the local coupling characteristic Γ_k:

$$\Gamma_k = |\mathcal{N}_a \cap \mathcal{B}| + |\mathcal{N}_b \cap \mathcal{A}| + |\mathcal{N}_a \backslash (\mathcal{A} \cup \mathcal{B})|, \tag{28}$$

for some $a \in \mathcal{A}$, $b \in \mathcal{B}$, with $\mathcal{A}, \mathcal{B}$ defined in (26). The global coupling characteristic Γ is defined as

$$\Gamma = \min_{k=1,\ldots,N-1} \Gamma_k. \tag{29}$$

Even though Γ_k are defined for some arbitrary $a \in \mathcal{A}$ and $b \in \mathcal{B}$, according to Lemma 3, it is independent of the specific choice of $a \in \mathcal{A}$ and $b \in \mathcal{B}$. Thus Γ_k, $k = 1, \ldots, N-1$ and Γ are well defined. Γ_k and Γ are defined for a specific choice of the chain refinement. Thus Γ may vary depending on the selected chain of refinement (25). For the network from Example 1, one can see, by simple observation, that the global coupling characteristics equals $\Gamma = 1$.

5.2.3. Main result on network synchronization

Theorem 4. *Consider N systems (1) interconnected with integral coupling (4) with the corresponding communication network graph $\mathcal{G}$. Suppose*

- *A1 system (1) is iSFP($-\gamma(s)$) with the corresponding functions $S(x)$ and $\rho(x)$ satisfying Assumption 1,*
- *A2 the graph $\mathcal{G}$ is sequentially decolorable with the corresponding global coupling characteristic Γ,*
- *A3 the nonlinear coupling gain $\lambda(s)$ is bounded, and satisfies the conditions[7] $\lambda(\cdot) \in L_1$ and*

$$\Gamma\lambda(s) \geq \gamma(s), \quad \forall s \in \mathbb{R}. \tag{30}$$

Then, for any set of initial conditions, all systems states $x_i(t)$, $i = 1, \ldots, N$, are bounded for $t \geq 0$ and asymptotically synchronize: $|x_i(t) - x_j(t)| \to 0$ as $t \to +\infty$ for all $i, j = 1, \ldots, N$.

See the Appendix for the proof. This theorem links together incremental feedback passivity properties [A1] and network properties [A2] through conditions on the nonlinear integral coupling with gain $\lambda(s)$ in [A3]. Condition [A1] can be verified using, for example, constructive results from Section 3.2 (Theorems 1 and 2). The network condition [A2] can be verified with simple algorithms based on the analysis presented in this section. The corresponding MATLAB code is available in Steur (2019). Once the chain of refinements corresponding to sequential decoloring of the network graph $\mathcal{G}$ is found, one can calculate the global coupling characteristic Γ and verify condition (30) in [A3].

The result of Theorem 4, in combination with previously presented constructive results, can be considered both as analysis and design tools. For design problems, as demonstrated by the example in Section 2.1, the nonlinear integral coupling with the minimal coupling "gain" $\lambda(s) = \gamma(s)/\Gamma$ can lead to more energy efficient synchronization with lower sensitivity to measurement noise. For analysis problems, the minimal nonlinear coupling gain $\lambda(s)$ can provide better understanding of the system dynamics and reveal new synchronization mechanisms, as will be demonstrated by an example in Section 6.

[7] One can avoid the condition $\lambda(\cdot) \in L_1$ in proving boundedness of the solutions by using the machinery of semi-passive systems (Pogromsky, 1998) for fixed bidirectional communication graphs. Interested readers are referred to Pavlov et al. (2009).

6. Illustrative example

Let us consider the FitzHugh–Nagumo (FHN) oscillator, which represents a simplified model of neuron dynamics (FitzHugh, 1961):

$$\begin{aligned} \dot{z}_i &= \tfrac{1}{\tau}(a + y_i - bz_i) + \tfrac{A_{ext}}{\tau}\cos\omega t =: q(z_i, y_i, t), \\ \dot{y}_i &= y_i - \tfrac{1}{3}y_i^3 - z_i + r + u_i =: p(z_i, y_i) + u_i, \end{aligned} \tag{31}$$

where y_i represents the membrane potential, z_i is an internal variable related to the ionic currents, and input u_i is used to establish coupling with other neurons. All other parameters are positive constants. For numerical simulations we choose the following values: $a = 0.7$, $b = 0.8$, $\tau = 100$, and $r = 0.3$. We added a common periodic forcing $\frac{A_{ext}}{\tau}\cos\omega t$ to the internal z_i-dynamics, which can make the neurons oscillate irregularly. (Note that for $a = b = 0$, we recover the dynamics of the forced Van Der Pol oscillator, which is known to behave chaotically for certain parameter values.) We take $A_{ext} = 0.03$ and $\omega = 0.026$.

We consider two cases of network topology: (a) two nodes interconnected with bi-directional coupling and (b) network topology from Fig. 4. Analysis of synchronization in a network of such oscillators with *linear* coupling is presented in Gorban, Jarman, Steur, van Leeuwen, and Tyukin (2015). Let us apply the theory developed in the previous sections and find a *nonlinear* integral coupling (4) that guarantees global exponential synchronization of networked identical oscillators (31). The analysis is based on Theorem 4, where we need to check conditions [A1] and [A2], then select coupling gain $\lambda(s)$ satisfying [A3].

[A1]: System (31) is iSFP($-\gamma(s)$) and satisfies Assumption 1: System (31) is of the form (10). Let us find $\gamma(s)$ for which this system is *iSFP*($-\gamma(s)$) with quadratic positive definite $S(x)$ and $\rho(x)$. Notice that the latter condition guarantees that Assumption 1 is satisfied. We find this $\gamma(s)$ using Theorem 2. Condition (11) is satisfied with $Q = [\tau]$, $M = [b]$. This particular choice of Q (and M) ensures that the right-hand side of inequality (12) is independent of z. Moreover, as $Q\frac{\partial q}{\partial y} + (\frac{\partial p}{\partial z})^T = 0$, we obtain $\tilde{\gamma}(s)$ from (12):

$$\tilde{\gamma}(s) \geq \epsilon + 1 - s^2 \quad \Rightarrow \quad \gamma(s) := \max\{0,\ \epsilon + 1 - s^2\}, \tag{32}$$

where $\epsilon > 0$ is an arbitrary parameter satisfying $\epsilon < b$ due to (13). For implementation, we select $\epsilon = 0.0001$.

[A2]: The communication network graph is sequentially decolorable. Both networks considered in this example (two bi-directionally coupled systems and six systems coupled as in Fig. 4) are sequentially decolorable with the corresponding minimal coupling characteristics equal to $\Gamma = 2$ (for 2 systems) and $\Gamma = 1$ (for 6 systems).

[A3]: Selection of the coupling gain $\lambda(s)$: As mentioned in the previous sections, we are interested in finding the smallest coupling that leads to synchronization. The structure of the smallest coupling gain $\lambda(s)$ can give insights into mechanisms of synchronization present in real systems. For design problems, it can lead to lower coupling actions needed to achieve synchronization, lower energy spent on coupling actions and lower sensitivity to noise. Therefore, we select the minimal $\lambda(s)$ according to the lower bound in (30): $\lambda(s) = \frac{1}{\Gamma}\gamma(s)$, $\forall s$. This choice of $\lambda(s)$ satisfies all conditions in [A3] of Theorem 4. Thus, all conditions of Theorem 4 are satisfied. This theorem guarantees that all solutions of the closed-loop system remain bounded for $t \geq 0$ and global asymptotic synchronization occurs for all systems/nodes in the network.

Simulation results for two bi-directionally coupled systems with initial conditions $[2, -4]^T$ and $[-1, 5]^T$ are presented in Fig. 7. The first three plots depict the states of the systems and the corresponding coupling actions (controls), and the last plot shows

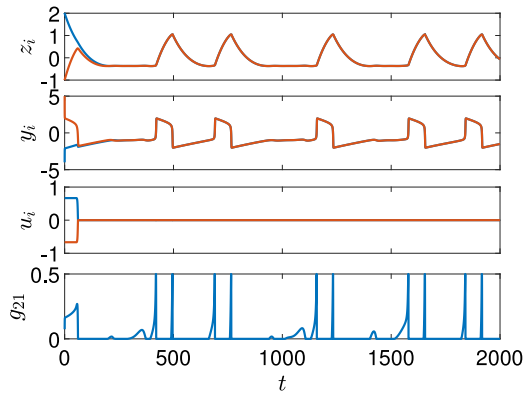

Fig. 7. Simulation results for two bi-directionally coupled FHN models: system states, controls and the variable coupling gain $g_{21}(t)$ between the 1st and 2nd system.

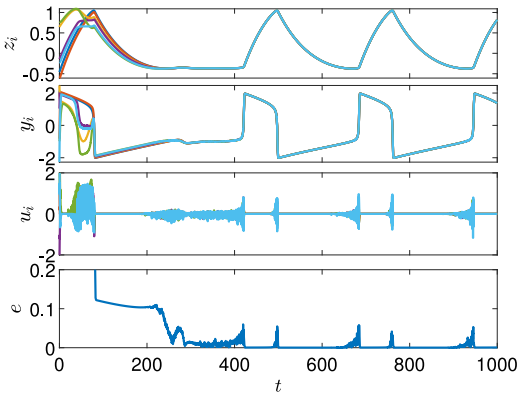

Fig. 8. Simulation result of the six nonlinearly coupled FHN neurons.

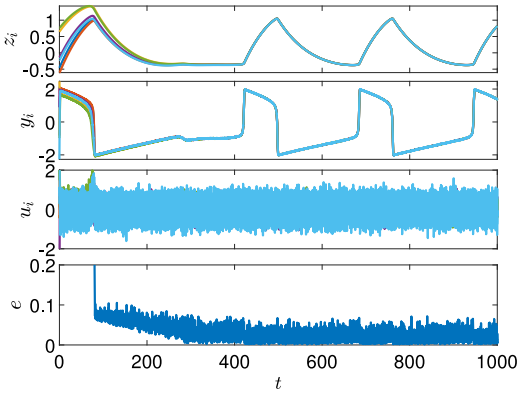

Fig. 9. Simulation result of the six linearly coupled FHN neurons.

the generalized variable gain $g_{21}(t)$ of the nonlinear integral coupling defined as $g_{21}(t) = \int_{y_2(t)}^{y_1(t)} \lambda(s)ds/(y_1(t)-y_2(t))$, Pavlov et al. (2009). We observe that the two systems rapidly synchronize. The generalized variable gain is most of the time equal to zero, indicating that no interaction is required. Only when the neuron spikes, the generalized variable gain is non-zero with a maximum of $(1+\epsilon)/2$. This variable gain (seen over the whole simulation period) is much lower than the best estimate of the synchronizing linear diffusive coupling gain we are aware of, which equals 0.5 (Gorban et al., 2015; Stan & Sepulchre, 2007). Lower coupling gains is a distinctive feature of the proposed method over linear diffusive couplings. Another feature of the proposed coupling is that it is bounded for all values y_1, y_2, which is not the case for linear diffusive coupling.

Interestingly, our proposed integral coupling turns out to generate a pulse-type of interaction, as demonstrated by the spiky generalized variable gain. The gain is zero most of the time and spikes only when the y variable jumps. This is a novel type of synchronizing interaction which turns to be more energy efficient and less sensitive to measurement noise, compared to linear diffusive couplings. This will be demonstrated by the next simulation with 6 systems and measurement noise.

In Fig. 8 we depict synchronization of six FHN oscillators interconnected as in Fig. 4 through the integral coupling with the minimal gain $\lambda(s) = \gamma(s)/\Gamma$ (note that in this case $\Gamma = 1$). We add noise to the outputs to simulate the effect of measurement noise. It is clearly visible in the inputs u_i and the synchronization error $e := \max_{i,j\in 1\ldots 6} |y_i - y_j|$ that this measurement noise only affects the dynamics when a spike in the outputs is either initiated or ended, i.e. when the generalized variable gain is non-zero. In Fig. 9 this simulation is repeated with linear coupling, $\lambda(s) \equiv 1+\epsilon$, which guarantees the same rate of convergence characterized by ϵ. Comparing the nonlinear and linear coupling results, we clearly see that the nonlinear coupling is less sensitive to measurement noise both in the control inputs u_i, and the steady-state synchronization errors e_i, at least, in L_1 and L_2 sense. The energy efficiency of the nonlinear integral coupling follows from comparing L_2 norms of the inputs for both the linear and nonlinear couplings: $\|u^{lin}\|_{L_2} = 18.9$, $\|u^{nl}\|_{L_2} = 10.6$. For the infinity norm, we have $\|u^{lin}\|_{L_\infty} = 10.0$, $\|u^{nl}\|_{L_\infty} = 2.7$. Similar relations were observed for various initial conditions. These results demonstrate the effectiveness of the selected nonlinear integral couplings also for the case of more complex network topologies. Another example demonstrating the effectiveness of the proposed approach can be found in Pavlov et al. (2018), where the developed theory was applied to Hindmarsh–Rose oscillators, in which not only the y-dynamics, but also the z-dynamics are nonlinear.

7. Conclusions

In this paper, we have considered the controlled synchronization problem for a class of identical nonlinear single-input–single-output systems[8] and proposed a novel nonlinear integral couplings design to achieve synchronization of systems on a class of interconnection networks. As demonstrated by the examples, the proposed nonlinear integral couplings with minimal gains (understood in a nonlinear sense) can lead to more efficient synchronization with lower input energy and lower sensitivity to measurement noise compared to conventional linear couplings. Application of the results to synchronization of FitzHugh–Nagumo oscillators revealed a novel type of synchronizing interaction, where synchronization is achieved and maintained through generically zero, but spiking coupling gains. From a design point of view, the obtained results give a constructive method to design nonlinear couplings and communication networks that render more efficient synchronization of the interconnected systems. From an analysis point of view, they can provide insight into potential nonlinear synchronization mechanisms in nature.

[8] An extension to the multiple-input–multiple-output case is possible by generalizing the iFP notion along the lines of Pavlov and Marconi (2008) and, under mild assumptions, our results cover specific cases of non-identical and uncertain systems, see Remark 2.

Acknowledgments

The authors would like to thank anonymous reviewers for their valuable comments, which helped to improve the paper, and Danila Semenov, Ph.D. student from St. Petersburg State University, Russia, for conducting initial simulations and analysis of the example from Section 6.

Appendix. Proofs

A.1. Proof of Lemma 1

Inequality (5) can be written in the form

$$\begin{aligned}&\frac{\partial S}{\partial x}(x_a-x_b)(f(x_a,t)+Bu_a-f(x_b,t)-Bu_b)\\&\le -\rho(x_a-x_b)+(y_a-y_b)\left(\int_{y_b}^{y_a}\gamma(s)ds+u_a-u_b\right),\end{aligned}$$

which holds for any x_a, x_b, u_a, u_b and $y_a = Cx_a, y_b = Cx_b$. For $x_a = x$, $u_a = u$, $x_b = 0$, $u_b = 0$, and after taking the term $\frac{\partial S}{\partial x}(x)f(0,t)$ to the right-hand side, we obtain

$$\begin{aligned}&\frac{d}{dt}S(x(t))=\frac{\partial S}{\partial x}(x)(f(x,t)+Bu)\\&\le -\rho(x)+y\left(\int_0^y\gamma(s)ds+u\right)+\frac{\partial S}{\partial x}(x)f(0,t)\\&\le -|x|\kappa(|x|)+|C\|x|\left(C_\gamma+C_u\right)+C_S|x\|f(0,t)|\\&\le -|x|(\kappa(|x|)-\underbrace{(|C|(C_\gamma+C_u)+C_sC_f)}_{=:L}).\end{aligned}\tag{A.1}$$

In this derivation we have utilized inequalities (7), (8), condition $\sup_{t\ge 0}|f(0,t)| =: C_f \le +\infty$, see (1), as well as inequalities on $|u(x,t)|$ and $\gamma(s)$ from the formulation of the lemma. Thus, $d/dtS(x(t)) \le 0$ for $|x| \ge \kappa^{-1}(L)$. This inequality, together with property (6), implies that the compact set $\{x : S(x) \le k_S\}$ is positively invariant for all $k_S > k_S^*$, for some $k_S^* > 0$. Since $S(x)$ is radially unbounded, for any initial condition of $x(0)$ there exists $k_S > k_S^*$ such that $x(t)$ lies in the compact positively invariant set $\{x : S(x) \le k_S\}$. □

A.2. Proof of Theorem 1

Consider system (1) written in an equivalent form:

$$\dot{x}=\tilde{f}(x,t)+B\int_0^y\tilde{\gamma}(s)ds+Bu,\quad y=Cx,\tag{A.2}$$

where $\tilde{f}(x,t) := f(x,t) - B\int_0^y\tilde{\gamma}(s)ds$. With this new notation, condition (9) is equivalent to

$$P\frac{\partial\tilde{f}}{\partial x}(x,t)+\frac{\partial\tilde{f}^T}{\partial x}(x,t)P\le -R\ \ \forall x\in\mathbb{R}^n,\ \ t\ge 0.\tag{A.3}$$

This matrix inequality implies (see, e.g. Demidovich (1967) and Pavlov et al. (2004)) that for any x_1, x_2 it holds that

$$(x_1-x_2)^TP(\tilde{f}(x_1,t)-\tilde{f}(x_2,t))\le -\frac{1}{2}(x_1-x_2)^TR(x_1-x_2).\tag{A.4}$$

Now consider the storage function $S(x) = 1/2x^TPx$. For any two solutions $x_1(t)$ and $x_2(t)$ of system (1) with inputs u_1, u_2 and outputs y_1, y_2:

$$\begin{aligned}&\frac{d}{dt}S(x_1(t)-x_2(t))\\&=(x_1-x_2)^TP\left(\tilde{f}(x_1,t)+B\left(\int_0^{y_1}\tilde{\gamma}(s)ds+u_1\right)\right)\\&\quad-(x_1-x_2)^TP\left(\tilde{f}(x_2,t)+B\left(\int_0^{y_2}\tilde{\gamma}(s)ds+u_2\right)\right)\\&=(x_1-x_2)^TP(\tilde{f}(x_1,t)-\tilde{f}(x_2,t))\\&\quad+(x_1-x_2)^TPB\left(\int_0^{y_1}\gamma(s)ds-\int_0^{y_2}\tilde{\gamma}(s)ds\right)\\&\quad+(x_1-x_2)^TPB(u_1-u_2)\\&\le -\frac{1}{2}(x_1-x_2)^TR(x_1-x_2)\\&\quad+(y_1-y_2)\left(\int_{y_2}^{y_1}\tilde{\gamma}(s)ds+u_1-u_2\right),\end{aligned}\tag{A.5}$$

where in the last inequality we utilized (A.4), equality $PB = C^T$ and the additive property of definite integrals. Taking into account the definition $\gamma(s) = \max\{0, \tilde{\gamma}(s)\}$, we obtain

$$\begin{aligned}&(y_1-y_2)\left(\int_{y_2}^{y_1}\tilde{\gamma}(s)ds\right)=(y_1-y_2)\left(\int_{y_2}^{y_1}\gamma(s)ds\right)\\&+(y_1-y_2)\left(\int_{y_2}^{y_1}\underbrace{\tilde{\gamma}(s)-\gamma(s)}_{\le 0}ds\right)\\&\le(y_1-y_2)\left(\int_{y_2}^{y_1}\gamma(s)ds\right)\end{aligned}\tag{A.6}$$

for all y_1, y_2. Substituting (A.6) into (A.5), we obtain (5) with quadratic $S(x) = 1/2x^TPx$ and $\rho(x) = 1/2x^TRx$. Thus, system (1) is *iFP*$(-\gamma(s))$. Moreover, if R is positive definite, then the system is *iSFP*$(-\gamma(s))$ and the functions $S(x)$ and $\rho(x)$ satisfy Assumption 1. □

A.3. Proof of Theorem 2

Choose the matrices P and R in (9) as

$$P:=\begin{bmatrix}Q & 0\\0 & 1\end{bmatrix},\quad R:=\begin{bmatrix}\epsilon I_{n-1} & 0\\0 & 2\epsilon\end{bmatrix}.$$

Notice that this P satisfies the equality $PB = C^T$. By combining all the terms in the first inequality in (9) in the right-hand side, one can see that for the chosen $P = P^T > 0$ and $R = R^T > 0$ this matrix inequality is equivalent to

$$J:=\begin{bmatrix}\mathcal{A} & \mathcal{M}\\\mathcal{M}^T & \mathcal{N}\end{bmatrix}\ge 0,\tag{A.7}$$

where

$$\mathcal{A}=-Q\frac{\partial q}{\partial z}-\frac{\partial q^T}{\partial z}Q-\epsilon I_{n-1},$$

$$\mathcal{M}=-Q\frac{\partial q}{\partial y}-\frac{\partial p^T}{\partial z},\quad \mathcal{N}=-2\frac{\partial p}{\partial y}+\tilde{\gamma}(y)-2\epsilon.$$

Due to (11), inequality (A.7) holds if

$$\tilde{J}:=\begin{bmatrix}M-\epsilon I_{n-1} & \mathcal{M}\\\mathcal{M}^T & \mathcal{N}\end{bmatrix}>0.\tag{A.8}$$

Recall that $\tilde{J}$ is positive definite if and only if $M - \epsilon I_{n-1} > 0$ and $\mathcal{N}-\mathcal{M}^T(M-\epsilon I_{n-1})^{-1}\mathcal{M} > 0$. The first inequality is guaranteed by (13), while the last one holds due to the choice of $\tilde{\gamma}(y)$ satisfying (12). Application of Theorem 1 concludes the proof. □

A.4. Proof of Lemma 3

Since $\mathcal{P}_{i_k}$ is a refinement of $\mathcal{P}_{i_{k+1}}$, every element of $\mathcal{P}_{i_k}$ is a subset of an element of $\mathcal{P}_{i_{k+1}}$. Since the number of elements (colors) in $\mathcal{P}_{i_{k+1}}$ is less than the number of elements (colors) in $\mathcal{P}_{i_k}$ by exactly 1, two elements from $\mathcal{P}_{i_k}$ will form one element

of $\mathcal{P}_{i_{k+1}}$. Let us denote these two elements by $\mathcal{A}$ and $\mathcal{B}$ and the remaining elements of the partition $\mathcal{P}_{i_k}$ by $\mathcal{C}_1, \dots, \mathcal{C}_l$ for some l. Then (26) holds. Let $a \in \mathcal{A}$ and $b \in \mathcal{B}$. Since $\mathcal{P}_{i_{k+1}}$ is a partition corresponding to relaxed balanced coloring, and $\mathcal{A} \cup \mathcal{B} \in \mathcal{P}_{i_{k+1}}$, then, by the definition of relaxed balanced coloring, for any two points $a, b \in \mathcal{A} \cup \mathcal{B}$, (27) holds. In particular, it holds for any $a \in \mathcal{A}$ and $b \in \mathcal{B}$.

Finally, since $\mathcal{P}_{i_k}$ is a partition corresponding to relaxed balanced coloring, for any $a_1, a_2 \in \mathcal{A}$, it holds that $\mathcal{N}_{a_1} \cap \mathcal{B} = \mathcal{N}_{a_2} \cap \mathcal{B}$ and $\mathcal{N}_{a_1} \cap \mathcal{C}_j = \mathcal{N}_{a_2} \cap \mathcal{C}_j$, for $j = 1, \dots, l$. Thus $|\mathcal{N}_a \cap \mathcal{B}|$, and $|\mathcal{N}_a \cap \mathcal{C}_j|$, and, in the same way, $|\mathcal{N}_b \cap \mathcal{A}|$ and $|\mathcal{N}_b \cap \mathcal{C}_j|$, $\forall j = 1, \dots, l$, are independent of the particular choice of $a \in \mathcal{A}$ and $b \in \mathcal{B}$. □

A.5. Proof of Theorem 4

Boundedness: Condition $\lambda(\cdot) \in L_1$ implies that $|u_i| \leq (N-1)\|\lambda(\cdot)\|_{L_1}$. In the same way, (30) and $\gamma(s) \geq 0$ (see Definition 2) imply that $\gamma(\cdot) \in L_1$. Thus, by Lemma 1, $x_i(t)$, $i = 1, \dots, N$, lie in a compact positive invariant set for all $t \geq 0$.

Synchronization: To prove synchronization in Theorem 4, we only need to demonstrate that each element of each partition $\mathcal{P}_{i_k}$, $k = 1, \dots, N$, is either an individual node, or a cluster of nodes that asymptotically synchronize. Since $\mathcal{P}_{i_N}$ contains only one element – the set of all nodes – this will prove asymptotic synchronization of all nodes in the network. We will show this by induction.

Induction base: Partition $\mathcal{P}_{i_0}$, consists of individual nodes.

Induction step: Suppose partition $\mathcal{P}_{i_k}$ contains either individual nodes or clusters of nodes that asymptotically synchronize. Let us show that $\mathcal{P}_{i_{k+1}}$ also consists of either individual nodes, or cluster of nodes that asymptotically synchronize. The structure of partitions $\mathcal{P}_{i_k}$ and $\mathcal{P}_{i_{k+1}}$ is specified in (26), Lemma 3. Thus we only need to show that $\mathcal{A} \cup \mathcal{B}$ consists of nodes with asymptotically synchronizing states. For simplicity of presentation, we consider the case of the partition $\mathcal{P}_{i_k}$ consisting of 3 elements: $\mathcal{P}_{i_k} = \{\mathcal{A}, \mathcal{B}, \mathcal{C}\}$. The case of more elements $\mathcal{C}_j$ in the partition or the case when $\mathcal{C}$ is empty can be proven by a minor modification. Since all nodes within $\mathcal{A}$ synchronize as well as all nodes within $\mathcal{B}$, it is enough to demonstrate that two nodes $a \in \mathcal{A}$ and $b \in \mathcal{B}$ synchronize, i.e. $|x_a(t) - x_b(t)| \to 0$ as $t \to +\infty$. Since $\mathcal{V} = \mathcal{A} \cup \mathcal{B} \cup \mathcal{C}$, by the definition of the integral coupling (4), we have

$$u_a = \sum_{j \in \mathcal{N}_a} \int_{y_a}^{y_j} \lambda(s)ds = \sum_{j \in \mathcal{N}_a \cap \mathcal{B}} \int_{y_a}^{y_j} \lambda(s)ds + \underbrace{\sum_{j \in \mathcal{N}_a \cap \mathcal{A}} \int_{y_a}^{y_j} \lambda(s)ds}_{*} + \sum_{j \in \mathcal{N}_a \cap \mathcal{C}} \int_{y_a}^{y_j} \lambda(s)ds. \tag{A.9}$$

Since nodes within $\mathcal{A}$, $\mathcal{B}$ and $\mathcal{C}$ synchronize, these nodes can be asymptotically represented by single nodes from the corresponding sets: $a \in \mathcal{A}$, $b \in \mathcal{B}$ and $c \in \mathcal{C}$. Thus

$$\sum_{j \in \mathcal{N}_a \cap \mathcal{B}} \int_{y_a}^{y_j} \lambda(s)ds = \sum_{j \in \mathcal{N}_a \cap \mathcal{B}} \left(\int_{y_a}^{y_b} \lambda(s)ds + \underbrace{\int_{y_b}^{y_j} \lambda(s)ds}_{*} \right),$$

$$\sum_{j \in \mathcal{N}_a \cap \mathcal{C}} \int_{y_a}^{y_j} \lambda(s)ds = \sum_{j \in \mathcal{N}_a \cap \mathcal{C}} \left(\int_{y_a}^{y_c} \lambda(s)ds + \underbrace{\int_{y_c}^{y_j} \lambda(s)ds}_{*} \right).$$

The integral terms marked with $*$ tend to zero, since the corresponding states (and outputs) synchronize (by the assumption that $\mathcal{A}$, $\mathcal{B}$ and $\mathcal{C}$ are (individually) synchronizing clusters) and since $\lambda(s)$ is bounded. Denoting the sum of these vanishing elements by ϵ_a, we can rewrite u_a from (A.9) and, in the same way, u_b as

$$u_a = |\mathcal{N}_a \cap \mathcal{B}| \int_{y_a}^{y_b} \lambda(s)ds + |\mathcal{N}_a \cap \mathcal{C}| \int_{y_a}^{y_c} \lambda(s)ds + \epsilon_a,$$
$$u_b = |\mathcal{N}_b \cap \mathcal{A}| \int_{y_b}^{y_a} \lambda(s)ds + |\mathcal{N}_b \cap \mathcal{C}| \int_{y_b}^{y_c} \lambda(s)ds + \epsilon_b.$$

Therefore,

$$u_a - u_b = \Gamma_k \int_{y_a}^{y_b} \lambda(s)ds + \epsilon_a - \epsilon_b, \tag{A.10}$$

with $\Gamma_k = (|\mathcal{N}_a \cap \mathcal{B}| + |\mathcal{N}_b \cap \mathcal{A}| + |\mathcal{N}_a \cap \mathcal{C}|)$. Notice that this Γ_k coincides with the one from Definition 6, since, in our case $\mathcal{N}_a \cap \mathcal{C} = \mathcal{N}_a \cap (\mathcal{A} \cup \mathcal{B})$. In (A.10), we also utilized the fact that $|\mathcal{N}_a \cap \mathcal{C}| = |\mathcal{N}_b \cap \mathcal{C}|$, see condition (27) in Lemma 3, and that $\int_{y_a}^{y_c} \lambda(s)ds - \int_{y_b}^{y_c} \lambda(s)ds = \int_{y_a}^{y_b} \lambda(s)ds$. Note that by the definition of the global coupling characteristic Γ (see Definition 6), inequality (30) from condition [A3] and (29) implies that

$$\Gamma_k \lambda(s) \geq \Gamma \lambda(s) \geq \gamma(s), \quad \forall s \in \mathbb{R}. \tag{A.11}$$

Substituting (A.10) into (5) and utilizing inequality (A.11) (note that in our case $\mathcal{N}_a \cap \mathcal{C} = \mathcal{N}_a \backslash (\mathcal{A} \cup \mathcal{B})$), we obtain

$$\frac{d}{dt} S(x_a(t) - x_b(t)) \leq -\rho(x_a - x_b) \quad + (y_a - y_b)(\epsilon_a - \epsilon_b). \tag{A.12}$$

By the conditions on the function $\rho(x)$, we have

$$\frac{d}{dt} S(x_a(t) - x_b(t)) \leq -\frac{1}{2}\rho(x_a - x_b) - |x_a - x_b| \left(\frac{1}{2}\kappa(x_a - x_b) - |\epsilon_a - \epsilon_b| \right).$$

Therefore, for $\frac{1}{2}\kappa(x_a - x_b) \geq |\epsilon_a - \epsilon_b|$ it holds that

$$\frac{d}{dt} S(x_a(t) - x_b(t)) \leq -\frac{1}{2}\rho(x_a - x_b). \tag{A.13}$$

This fact, together with conditions on function $S(x)$ implies, through an incremental ISS argument (Angeli, 2002), that vanishing $\epsilon_a(t) - \epsilon_b(t)$ (as both $\epsilon_a(t)$ and $\epsilon_b(t)$ vanish) yields $|x_a(t) - x_b(t)| \to 0$ as $t \to +\infty$. This completes the proof of the induction step that $\mathcal{P}_{i_{k+1}}$ also consists of either individual nodes, or clusters of nodes that asymptotically synchronize, and thus concludes the proof of the theorem. □

References

Abrams, D. M., Pecora, L. M., & Motter, A. E. (2016). Introduction to focus issue: Patterns of network synchronization. *Chaos*, *26*(094601).

Aguiar, M. A. D., & Dias, A. P. S. (2014). The lattice of synchrony subspaces of a coupled cell network: Characterization and computation algorithm. *Journal of Nonlinear Sciences*, *24*(6), 949–996.

Andreasson, M., Dimarogonas, D. V., Sandberg, H., & Johansson, K. H. (2014). Distributed control of networked dynamical systems: Static feedback, integral action and consensus. *IEEE Transactions on Automatic Control*, *59*(7), 1750–1764.

Angeli, D. (2002). A Lyapunov approach to incremental stability properties. *IEEE Transactions on Automatic Control*, *47*, 410–421.

Arcak, M. (2007). Passivity as a design tool for group coordination. *IEEE Transactions on Automatic Control*, *52*(8), 1380–1390.

Belykh, I., & Hasler, M. (2011). Mesoscale and clusters of synchrony in networks of bursting neurons. *Chaos*, *21*(1).

Belykh, I. V., & Porfiri, M. (2016). Introduction: Collective dynamics of mechanical oscillators and beyond. *Chaos*, *26*.

Birkhoff, G. (1948). *Lattice theory* (Revised ed.). New York, NY: American Mathematical Society.
Cardoso, D. M., Delorme, C., & Rama, P. (2007). Laplacian eigenvectors and eigenvalues and almost equitable partitions. *European Journal of Combinatorics*, *28*(3), 665–673.
Caroll, T., & Pecora, L. (1991). Synchronizing chaotic circuits. *IEEE Transacitons on Circuits Systems – I: Fundamental Theory and Applications*, *38*, 453–456.
Chopra, N., & Spong, M. (2008). Output synchronization of nonlinear systems with relative degree one. In H. Vincent, D. Blondel, & S. Boyd (Eds.), *Recent advances in learning and control* (pp. 51–64). New York:Springer-Verlag.
Demidovich, B. P. (1967). *Lectures on stability theory (in Russian)*. Moscow: Nauka.
Dimarogonas, D. V., & Kyriakopoulos, K. J. (2008). Connectedness preserving distributed swarm aggregation for multiple kinematic robots. *IEEE Transactions on Robotics*, *24*(5), 1213–1223.
Dörfler, F., & Bullo, F. (2014). Synchronization in complex networks of phase oscillators: A survey. *Automatica*, *50*(6), 1539–1564.
Dörfler, F., Chertkov, M., & Bullo, F. (2013). Synchronization in complex oscillator networks and smart grids. *Proceedings of the National Academy of Sciences of the United States of America*, *110*(6), 2005–2010.
El-Gohary, A. (2006). Optimal synchronization of Rössler system with complete uncertain parameters. *Chaos, Solitons & Fractals*, *27*, 345–355.
Fazlyab, M., Dörfler, F., & Preciado, V. M. (2017). Optimal network design for synchronization of coupled oscillators. *Automatica*, *84*, 181–189.
FitzHugh, R. (1961). Impulses and physiological states in theoretical models of nerve membrane. *Biophysical Journal*, *1*, 445–466.
Fradkov, A. L., & Pogromsky, A. Y. (1998). *Introduction to control of oscillations and chaos*. Singapore: World Scientific.
Gambuzza, L. V., & Frasca, M. (2019). A criterion for stability of cluster synchronization in networks with external equitable partitions. *Automatica*, *100*, 212–218.
Golubitsky, M., Stewart, I., & Török, A. (2005). Patterns of synchrony in coupled cell networks with multiple arrows. *SIAM Journal on Applied Dynamical Systems*, *4*(1), 78–100.
Gorban, A. N., Jarman, N., Steur, E., van Leeuwen, C., & Tyukin, I. Y. (2015). Leaders do not look back, or do they? *Mathematical Modelling of Natural Phenomena*, *10*(3), 212–231.
Hamadeh, A., Stan, G.-B., Sepulchre, R., & Goncalves, J. (2012). Global state synchronization in networks of cyclic feedback systems. *IEEE Transactions on Automation Control*, *57*(2), 478–483.
He, G., & Yang, J. (2008). Adaptive synchronization in nonlinearly coupled dynamical networks. *Chaos, Solitons & Fractals*, *38*(5), 1254–1259.
Ji, M., & Egerstedt, M. (2007). Distributed coordination control of multiagent systems while preserving connectedness. *IEEE Transactions on Robotics*, *23*(4), 693–703.
Khalil, H. K. (1996). *Nonlinear systems* (2nd ed.). Upper Saddle River: Prentice-Hall.
Levine, J. (2004). On the synchronization of a pair of independent windshield wipers. *IEEE Transactions on Control Systems Technology*, *12*(5), 787–795.
Liu, X., & Chen, T. (2008). Synchronization analysis for nonlinearly-coupled complex networks with an asymmetrical coupling matrix. *Physica A. Statistical Mechanics and its Applications*, *387*(16-17), 4429–4439.
Liu, Y.-C., & Chopra, N. (2012). Controlled synchronization of heterogeneous robotic manipulators in the task space. *IEEE Transactions on Robotics*, *28*(1), 268–275.
Liu, X., & Iwasaki, T. (2017). Design of coupled harmonic oscillators for synchronization and coordination. *IEEE Transactions on Automatic Control*, *62*(8), 3877–3889.
Liu, Z., Saberi, A., Stoorvogel, A. A., & Nojavanzadeh, D. (2020). H_∞ almost state synchronization for homogeneous networks of non-introspective agents: A scale-free protocol design. *Automatica*, *122*.
Macellari, L., Karayiannidis, Y., & Dimarogonas, D. V. (2017). Multi-agent second order average consensus with prescribed transient behavior. *IEEE Transactions on Automatic Control*, *62*(10), 5282–5288.
Modares, H., Lewis, F. L., Kang, W., & Davoudi, A. (2018). Optimal synchronization of heterogeneous nonlinear systems with unknown dynamics. *IEEE Transactions on Automatic Control*, *63*(1), 117–131.
Nijmeijer, H., & Mareels, I. (1996). An observer looks at synchronization. *IEEE Transactions on Circuit Systems. I*, *44*, 882–890.
Nijmeijer, H., & Rodriguez-Angeles, A. (2003). *Synchronization of mechanical systems*. World Scientific.
Nishikawa, T., & Motter, A. E. (2006). Maximum performance at minimum cost in network synchronization. *Physica D*, *224*(1), 77–89.
Notarstefano, G., & Parlangeli, G. (2013). Controllability and observability of grid graphs via reduction and symmetries. *IEEE Transactions on Automatic Control*, *58*(7), 1719–1731.
Oud, W. T., & Tyukin, I. (2004). Sufficient conditions for synchronization in an ensemble of Hindmarsh and Rose neurons: passivity-based approach. In *Proc. of 6th IFAC symposium on nonlinear control systems*.
Panteley, E., & Loría, A. (2017). Synchronization and dynamic consensus of heterogeneous networked systems. *IEEE Transactions on Automatic Control*, *62*(8), 3758–3773.
Pavlov, A., & Marconi, L. (2008). Incremental passivity and output regulation. *Systems & Control Letters*, *57*, 400–409.
Pavlov, A., Pogromsky, A., van de Wouw, N., & Nijmeijer, H. (2004). Convergent dynamics, a tribute to Boris Pavlovich Demidovich. *Systems & Control Letters*, *52*, 257–261.
Pavlov, A., Proskurnikov, A., Steur, E., & van de Wouw, N. (2018). Synchronization of networked oscillators under nonlinear integral coupling. In *Proc. 5th IFAC conference on analysis and control of chaotic systems*, Eindhoven.
Pavlov, A., Steur, E., & van de Wouw, N. (2009). Controlled synchronization via nonlinear integral coupling. In *Proc. 48th IEEE conference on decision and control*, Shanghai, China.
Pavlov, A., van de Wouw, N., & Nijmeijer, H. (2005). *Uniform output regulation of nonlinear systems: a convergent dynamics approach*. Boston: Birkhauser.
Pogromsky, A. (1998). Passivity based design of synchronizing systems. *International Journal of Bifurcation and Chaos*, *8*(2), 295–319.
Poonawala, H. A., & Spong, M. W. (2017). Preserving strong connectivity in directed proximity graphs. *IEEE Transactions on Automatic Control*, *62*(9), 4392–4404.
Proskurnikov, A. (2013). Consensus in switching networks with sectorial nonlinear couplings: Absolute stability approach. *Automatica*, *49*(2), 488–495.
Proskurnikov, A. V. (2014). Nonlinear consensus algorithms with uncertain couplings. *Asian Journal of Control*, *16*(5), 1277–1288.
Proskurnikov, A. V., & Cao, M. (2017). Synchronization of Goodwin's oscillators under boundedness and nonnegativeness constraints for solutions. *IEEE Transactions on Automatic Control*, *62*(1), 372–378.
Ramirez, J. P., Olvera, L. A., Nijmeijer, H., & Alvarez, J. (2016). The sympathy of two pendulum clocks: beyond Huygens' observations. *Scientific Reports*, *6*(23580).
Saber, R. O., & Murray, R. M. (2003). Consensus protocols for networks of dynamic agents. In *Proc. American control conference, Vol. 2* (pp. 951–956).
Stan, G.-B., & Sepulchre, R. (2007). Analysis of interconnected oscillators by dissipativity theory. *IEEE Transactions on Automatic Control*, *52*(2), 256–270.
Steur, E. (2019). Matlab code for calculation of Hasse diagrams. post= [online; accessed 29-april-2019],. https://www.dcsc.tudelft.nl/esteur/software/synchronysubspaces/.
Steur, E., & Nijmeijer, H. (2011). Synchronization in networks of diffusively time-delay coupled (semi-)passive systems. *IEEE Transactions on Circuit Systems I: Regular Papers*, *58*(6), 1358–1371.
Steur, E., Ünal, H., van Leeuwen, C., & Michiels, W. (2016). Characterization and computation of partial synchronization manifolds for diffusive delay-coupled systems. *SIAM Journal on Applied Dynamical Systems*, *15*(4), 1874–1915.
Stoorvogel, A. A., Saberi, A., & Zhang, M. (2017). Solvability conditions and design for state synchronization of multi-agent systems. *Automatica*, *84*, 43–47.
Strogatz, S. H. (2000). From Kuramoto to Crawford: exploring the onset of synchronization in populations of coupled oscillators. *Physica D*, *143*.
Strogatz, S. H. (2003). *Sync: The emerging science of spontaneous order*. Hachette Books.
Tuna, S. E. (2017). Synchronization of harmonic oscillators under restorative coupling with applications in electrical networks. *Automatica*, *75*, 236–243.
Yu, W., Chen, G., & Cao, M. (2011). Consensus in directed networks of agents with nonlinear dynamics. *IEEE Transactions on Automatic Control*, *56*(6), 1436–1441.
Yu, W., Chen, G., Cao, M., & Kurths, T. (2010). Second order consensus for multiagent systems with directed topologies and nonlinear dynamics. *IEEE Transactions on Systems, Man, Cybernetics, Part B (Cybernetics)*, *40*(3), 881–891.
Zhang, F., Trentelman, H. L., & Scherpen, J. M. A. (2014). Fully distributed robust synchronization of networked Lur'e systems with incremental nonlinearities. *Automatica*, *50*(10), 2515–2526.

Alexey Pavlov obtained his M.Sc.-degree (cum laude) in Applied Mathematics from St. Petersburg State University, Russia, and Ph.D.-degree in Mechanical Engineering from Eindhoven University of Technology, The Netherlands in 1998 and 2004, respectively. Currently he holds a full professor position at the Department of Geoscience and Petroleum of the Norwegian University of Science and Technology (NTNU). He held various academic and industrial positions at the Institute for Problems of Mechanical Engineering, Russia (1999), Ford Research Laboratory, USA (2000), Eindhoven University of Technology (2005), NTNU (2005–2009), Equinor Research Centre, Norway (2009–2016). He published the book 'Uniform Output Regulation of Nonlinear Systems: A convergent Dynamics Approach' with N. van de Wouw and H. Nijmeijer (Birkhauser, 2005). He received the IEEE Control Systems Technology Award (2015) "For the development and application of variable-gain control techniques for high-performance motion systems" and IFAC World Congress Best Application Paper Award (2011) for the work "Drilling

seeking automatic control solutions". His inventions within automatic optimization are implemented in several oil production fields. His current research interests include control of nonlinear systems, control and optimization of highly uncertain systems, automation and digitalization in the energy industry and various industrial applications of automatic control and optimization.

Erik Steur obtained his M.Sc.-degree (cum laude) and Ph.D.-degree from Eindhoven University of Technology (TU/e), in 2007 and 2011, respectively. He currently is an assistant professor at the department of Mechanical Engineering of TU/e, and one of the leaders of the Grip on Complexity pillar of the Institute for Complex Molecular Systems at TU/e. He was an assistant professor at Delft University of Technology from 2017–2019 and held postdoctoral research positions at TU/e (2015–2017) and KU Leuven (2012–2015). His core expertise is on the modeling and analysis of collective dynamics – in particular, cluster synchronization and pattern generation – of networked systems, with applications to neuroscience and chemistry. He has co-organized several international conferences. He currently serves as associate editor for Systems and Control Letters, and Communications in Nonlinear Science and Numerical Simulation (from January 2022).

Nathan van de Wouw obtained his M.Sc.-degree (with honors) and Ph.D.-degree in Mechanical Engineering from the Eindhoven University of Technology, the Netherlands, in 1994 and 1999, respectively. He currently holds a full professor position at the Mechanical Engineering Department of the Eindhoven University of Technology, the Netherlands. He has been working at Philips Applied Technologies, The Netherlands, in 2000 and at the Netherlands Organization for Applied Scientific Research, The Netherlands, in 2001. He has been a visiting professor at the University of California Santa Barbara, U.S.A., in 2006/2007, at the University of Melbourne, Australia, in 2009/2010 and at the University of Minnesota, U.S.A., in 2012 and 2013. He has held a (part-time) full professor position at the Delft University of Technology, the Netherlands, in 2015–2019. He has also held an adjunct full professor position at the University of Minnesota, U.S.A, in 2014–2021. He has published the books 'Uniform Output Regulation of Nonlinear Systems: A convergent Dynamics Approach' with A. Pavlov and H. Nijmeijer (Birkhauser, 2005) and 'Stability and Convergence of Mechanical Systems with Unilateral Constraints' with R.I. Leine (Springer-Verlag, 2008). In 2015, he received the IEEE Control Systems Technology Award "For the development and application of variable-gain control techniques for high-performance motion systems". He is an IEEE Fellow for his contributions to hybrid, data-based and networked control.